49 8-15-95 JS ②

PREPARED FOR THE U.S. DEPARTMENT OF ENERGY,
UNDER CONTRACT DE-AC02-76-CHO-3073

PPPL-3011-R
UC-420,422,426

PPPL-3011-R

COLLISIONAL STOCHASTIC RIPPLE DIFFUSION OF ALPHA PARTICLES AND BEAM IONS ON TFTR

BY

M.H. REDI, M.C. ZARNSTORFF, R.B. WHITE, ET AL.

JULY 1995

PPPL PRINCETON PLASMA PHYSICS LABORATORY

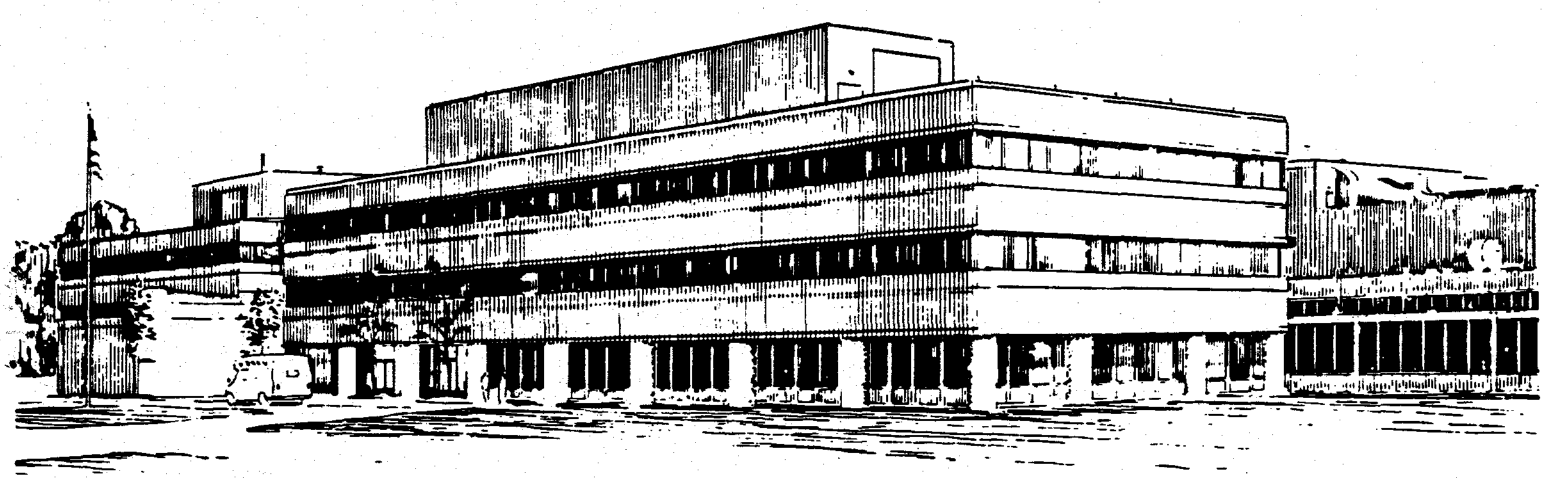

PRINCETON UNIVERSITY, PRINCETON, NEW JERSEY

NOTICE

This report was prepared as an account of work sponsored by an agency of the United States Government. Neither the United States Government nor any agency thereof, nor any of their employees, makes any warranty, express or implied, or assumes any legal liability or responsibility for the accuracy, completeness, or usefulness of any information, apparatus, product, or process disclosed, or represents that its use would not infringe privately owned rights. Reference herein to any specific commercial produce, process, or service by trade name, trademark, manufacturer, or otherwise, does not necessarily constitute or imply its endorsement, recommendation, or favoring by the United States Government or any agency thereof. The views and opinions of authors expressed herein do not necessarily state or reflect those of the United States Government or any agency thereof.

NOTICE

This report has been reproduced from the best available copy.
Available in paper copy and microfiche.

Number of pages in this report: 65

DOE and DOE contractors can obtain copies of this report from:

Office of Scientific and Technical Information
P.O. Box 62
Oak Ridge, TN 37831;
(615) 576-8401.

This report is publicly available from the:

National Technical Information Service
Department of Commerce
5285 Port Royal Road
Springfield, Virginia 22161
(703) 487-4650

DISCLAIMER

Portions of this document may be illegible in electronic image products. Images are produced from the best available original document.

Collisional Stochastic Ripple Diffusion of Alpha Particles and Beam Ions on TFTR

M. H. Redi, M. C. Zarnstorff, R. B. White, R. V. Budny,

A. C. Janos, D. K. Owens, J. F. Schivell, S. D. Scott, S. J. Zweben

Princeton Plasma Physics Laboratory,

Princeton University, P. O. Box 451

Princeton, NJ 08543

Abstract

Predictions for ripple loss of fast ions from TFTR are investigated with a guiding center code including both collisional and ripple effects. A synergistic enhancement of fast ion diffusion is found for toroidal field ripple with collisions. The total loss is calculated to be roughly twice the sum of ripple and collisional losses calculated separately. Discrepancies between measurements and calculations of plasma beta at low current and large major radius are resolved when both effects are included for neutral beam ions. A 20–30% reduction in alpha particle heating is predicted for $q_a = 6 - 14$, R = 2.6 m DT plasmas on TFTR due to first orbit and collisional stochastic ripple diffusion.

DISTRIBUTION OF THIS DOCUMENT IS UNLIMITED

MASTER

1. Introduction

There has been considerable recent experimental and theoretical interest in the ripple and collisional loss of fast ions in high temperature tokamak fusion plasmas [1–27]. Pioneering work by Tani[21–23], White[7–9], and others have made possible extensive computations which include both collisional and ripple loss processes, in spite of numerical difficulties. Efforts to include both effects for specific tokamak experiments have, up to this point, been limited to calculations for a few cases on JT-60U [17, 26] and JET [25]. Similar extensive computations [21–23] as well as approximate analytic treatments [6] have also been carried out for future reactors such as ITER and INTOR.

This is an important issue for the design of future tokamak reactors such as ITER because stochastic ripple diffusion of alpha particles deposits a strongly localized heat load on the first wall. Thus, in addition to clarifying questions about heat and particle transport, verification of code calculations of fast ion transport by comparison with experiment provides support for the design of future fusion devices. Here we carry out a detailed computational study for TFTR including both collisional and ripple transport effects for neutral beam ions in high q_a plasmas and for alpha particles in projected DT experiments.

Transport analysis of low current, large major radius plasmas on TFTR has led to unexplained discrepanies between the measured and kinetically calculated stored plasma energies. The discrepancy in beta is found to increase with major radius and with reduced plasma current. The relatively poor performance of large major radius supershots at low Ip reflects this unexplained energy loss, which ranges from 10 to 40% of beta as calculated by the PPPL analysis codes SNAP [28] and TRANSP [29]. The SNAP analysis is time independent not including collisional orbit loss effects, while time dependent TRANSP analysis has not previously included ripple loss calculations. Clarification of this is particularly important for understanding ICRH minority heated plasma transport, since ICRH heating must be carried out in large major radius plasmas for good antenna-plasma coupling. Low triton burnup measurements on TFTR, $1/2 \pm 1/4$ classical expectations [30], also may be due to stochastic ripple loss.

Stochastic ripple losses were hypothesized to be responsible for the beta discrepancies by causing anomalously large losses of trapped neutral beam ions. Ripple losses of fast ions have been shown to cause significant losses on the ISX-B [11], JT-60U [17, 26], JET [18, 19, 25] and TORE SUPRA [20] tokamaks. The magnetic geometry of TFTR leads to negligible ripple trapping losses of energetic ions (with the exception of recent TAE-assisted ripple trapped losses of rf ions).

This simulation study is carried out with a Hamiltonian guiding center drift orbit Monte Carlo code, ORBIT, developed by White and Chance [7], based on the canonical Hamiltonian guiding center variables of White [8]. Because of computational requirements only a few plasmas have been analysed with this method. These cases are intended to serve as benchmarks and guides in routine transport analysis, which will make use of faster, approximate models. Previous estimates of expected alpha losses from high current TFTR discharges were calculated with ripple alone or with collisions alone and were found to be about 5-10% [12-14]. Over a decade ago the importance of collisional effects on alpha particle losses was pointed out by Tani [23]. Recent advances in computational hardware and software have made possible the present quantitative work.

Sections 2 and 3 discuss the physics of stochastic ripple diffusion, details of the ORBIT code, and the simulation procedure. In Sec. 4, the experiments simulated are presented. In Sec. 5, results are compared with the experimental beta discrepancies for neutral beam ions. Particle losses are calculated for both neutral beam ions and alpha particles. Section 6 covers toroidal field-error-dependent stochastic diffusion losses and in Sec. 7 a summary and conclusion are presented.

2. Collisional Stochastic Ripple Loss Physics

2.1. Stochastic Ripple Loss Criterion

A simple, rough estimate for the stochastic ripple diffusion-free domain for specific experiments has been derived by Goldston, White and Boozer [5]. They have derived a threshold for stochastic ripple loss

$$\delta_s = (\epsilon/(N\pi q))^{1.5}(1/\rho q')$$

where ϵ = inverse aspect ratio, N = number of coils, q is the plasma safety factor, q′ = dq/dr and ρ is the ion Larmor radius. δ, The toroidal field ripple is defined $\delta = (B_{MAX} - B_{MIN})/(B_{MAX} + B_{MIN})$, where B_{MAX} and B_{MIN} are the maximum and minimum field magnitudes at constant major radius and elevation. Trapped ions whose turning point lies in a region where δ exceeds the threshold δ_s are subject to stochastic ripple diffusion. An empirical factor of 1/2 has often been included in the stochastic ripple loss criterion [11, 12], although Boivin found that the pitch angle dependence of fusion product protons on TFTR was in better agreement with the original published criterion. In Sec. 5.1 the stochastic diffusion free regions are shown for each experiment modelled. The criterion was derived in a zero banana width, low β, cylindrical approximation. Finite orbit width effects on stochastic ripple diffusion have recently been addressed for JET [27], where the stochastic threshold of high energy ions is found to undergo significant modification. Most ions affected would have been stochastic ripple lost anyway so that the number of stochastically moving particles is only slightly different. ORBIT simulations follow each ion orbit in detail until it leaves the plasma. Comparative results will be used to evaluate the normalization of the δ_s model for TFTR in a separate paper.

2.2. Ion Pitch Angle Dependence

Ripple and first orbit ion losses are strongly dependent on ion pitch angle. The distribution in pitch determines the trapped fraction. When a banana-trapped ion is near the bounce point (where $v_{//} = 0$), it is most strongly affected by the nonaxisymmetric tokamak magnetic field.

In Ref. [12], Boivin plotted the topology of the magnetic moment and turning point radius dependence for trapped, passing, first orbit lost and stochastic ripple lost 3 Mev protons for a 1.4 MA TFTR plasma. The details of the plot will change with variation in ion energy, plasma current, major radius, *etc.* but the topology will not. Figure 1 is a sketch based on that figure which shows the phase space occupied by trapped and passing ions, characterized by μ/μ_o and a normalized minor radius crossing point (where the orbit crosses the midplane on the low field side). The first-orbit lost counter-passing particles are included in the first-orbit lost trapped particle category as they are born counter-passing and after a bounce becoming co-passing. Here μ is the ion magnetic moment and $\mu_o = E_o/B_o$, with E_o being the birth energy and B_o the magnetic field at the magnetic axis. Separate regions of this phase space are occupied by passing and trapped ions, with the trapped ions found in regions characterized by first orbit loss, TF ripple stochastic loss or confined orbits. This picture is helpful in visualizing the different physical processes affecting the fast ions under study. In particular, pitch angle scattering causes trapped (and passing) ions to move into the stochastic ripple and first orbit loss domains as μ is changed.

3. Guiding Center Code ORBIT Simulations

To test whether ripple losses are significant on TFTR, a Monte Carlo Hamiltonian coordinate drift orbit guiding center code, ORBIT [7], was used with minor modifications. The code was run with plasma equilibrium flux surfaces generated by the PEST equilibrium code [32, 33]. Plasma pressure and q profiles from TRANSP simulations of specific TFTR experiments, were input to the PEST code. The equilibrium was then mapped into the Hamiltonian coordinates used by the guiding center code.

The guiding center code was used to follow 256 orbiting particles in a magnetic geometry given by

$$B = B(\Psi, \theta)(1 + \delta(\Psi, \theta) sin N\phi)$$

with $B(\Psi,\theta)$ from the PEST equilibrium after a transformation to Boozer coordinates. Magnetic flux coordinate definitions are described in detail in Refs. [7-9]. Ψ is the poloidal magnetic flux surface coordinate, θ the poloidal angle and ϕ the toroidal angle. The ripple amplitude $\delta(R,Z)$ is given by [12]

$$\delta = \delta_o exp\{[(R-R_{rip})^2 + b_{rip}(Z)^2]^{1/2}/w_{rip}\}.$$

This function is fit using splines in the (Ψ,θ) plane. The coefficients R_{rip}, b_{rip}, δ_o and w_{rip} were fit to the calculated vacuum ripple. Here R_o is the plasma major radius, $R_{rip} = 2.25$ m is the major radius of the center of the ripple, $b_{rip} = 1.1$ is the ellipticity, δ_o is 0.000014 and $w_{rip} = 0.185$ m is the ripple scale length. There are N = 20 toroidal field coils on TFTR. Ripple on TFTR increases to about $\delta = 2\%$ at the tokamak outer midplane wall. Figure 2 shows contours of TFTR toroidal field ripple strength.

In our simulations, neutral beam and alpha orbits were followed with pitch angle scattering and energy slowing down effects. Collision rates were evaluated near the magnetic axis, using formulae for pitch angle scattering ($\nu_{PA} = \nu_\perp/2$) and slowing down processes as given in Ref. [31]. The effect of radial variation of the rates is discussed in Sec. 5.4.4.

The particle distributions were generated by Monte Carlo techniques. The neutral beam fast ion input profiles for each experiment were obtained from total beam deposition profiles calculated by TRANSP. Identical beam source profiles were used for all tangency radii. Alpha particle simulations assumed a model source profile, similar to that calculated by TRANSP in predicting high power supershot DT experiments.

Although the neutral beam production process causes about 20% of the beam power to be deposited in half energy and one third energy particles, only ions with full initial energies were simulated. Particles reaching the last closed flux surface were defined as lost. Total losses were integrated over a full energy slowing down time, τ_ϵ^α, for alpha particles and over half of an energy slowing down time, τ_ϵ^{nb}, for neutral beam ions.

Initial and final lost particle parameters were gathered in a database (out of a total of 256 ions for alpha simulations and for each beam line in neutral beam simulations), and the behavior of prompt and delayed ion losses as well as individual ion orbits, were studied. Simulations with collisions and ripple turned on separately were carried out to investigate the relative effectiveness of each transport process. The guiding center code includes orbit calculations for both stochastic ripple lost and ripple-trapped [10] losses.

4. TFTR Experiments Simulated

Plasma parameters for the four TFTR experiments for which fast ion orbits were followed are shown in Table I. E_{nb} is the first component of the injection beam energy for each experiment. Three of the experiments, with plasma currents of 0.9, 1.0 and 1.8 MA had major radius 2.6 m, while the fourth experiment, a high performance supershot, was carried out at 1.6 MA and major radius 2.45 m, similar to that studied in Ref. [34]. Neutral beam orbits were simulated for the R = 2.6 m cases at I_P = 0.9 and 1.0 MA. Alpha simulations were carried out for scenarios at low and high current as well as small and large major radius.

The low current experiments for which neutral beam ion orbits were simulated were designed for study of the plasma q profile, with large bootstrap current fractions. Comparison of magnetically measured plasma beta to kinetic beta calculations in TRANSP lead to beta discrepancies of 28% for the experiment at 0.9 MA and 8% for the experiment at 1.0 MA (Table I). The two experiments were characterized by different fractions of co-injected (injection direction parallel to I_P) and counter-injected ions. The neutral beam ions for the experiment at 0.9 MA were injected along six lines of sight with tangency radii given by R_T = -2.29, -1.99, -1.74 m for counter-injected ions and 2.23, 1.99, 1.80 m for co-injected ions, where R_T is the distance of closest approach to the tokamak center. Counter-injected ions are subject to signficantly higher first orbit losses than co-injected ions, for most of which the unperturbed orbits lie within the last closed flux surface. The Larmor radius for the 95.2 kev full energy deuterium ions is $\approx$ 1 cm and for alpha particles is $\approx$ 6 cm. The banana widths, proportional to q, are quite wide for the 0.9 MA experiment; the fattest banana width being $q\rho\sqrt{2/\epsilon}$, approximately equal to 35 cm for beam ions at the plasma edge.

In Table II are shown simulation parameters for the neutral beam and alpha particle orbits studied, including pitch angle scattering collision rates and energy slowing down times. In the table, τ_{tran} is the toroidal transit time of a fast ion at the magnetic axis with pitch $v_{//}/v$ = 1. The source distribution in pitch is given by

$$v_{//}/v = R_T/R$$

for neutral beam ions at the point of deposition and is isotropic for alphas.

Alpha particle orbits were also simulated for the I_P = 0.9 MA, R = 2.6 m case, as well as for two other typical TFTR experiments. These other scenarios, similar to DT experiments, were a no-ICRH baseline case at I_P = 1.8 MA, R =2.6 m and a high power supershot at I_P

= 1.6 MA, R = 2.45 m. Model alpha profiles were assumed and simulations were carried out for these experimental scenarios, although the original experiments were deuterium only. Simulations for the 1993-1994 TFTR DT experiments [35, 36] are in preliminary stages and will be published separately.

5. Results and Discussion

5.1. Stochastic Diffusion Free Domains

Contours in Fig. 3 bound the stochastic diffusion-free regions, for $\delta/\delta_s = 0.25, 0.5, 1.0$ criteria obtained with the Goldston, White, Boozer model. Contours are shown for fast neutral beam ions and alpha particles for experiments at 0.9 MA and 2.6 m (3a, 3b), at 1.6 MA and 2.45 m (3c, 3d), as well as for neutral beam ions and alpha particles at 1.8 MA and 2.6 m (3e, 3f). These thresholds are for trapped ions with turning points in the indicated regions and with velocity equal to the inital velocity. We see that ripple is not expected to cause neutral beam losses for the R = 2.45 m case and that there is a much larger region free of stochastic ripple diffusion for alphas for this shot (Fig. 3d), compared to the low current experiment at 2.6 m (Fig. 3b), for which the model predicts a vanishingly small stochastic free region. The toroidal field ripple is smaller for plasmas with vacuum magnetic field axis at small major radius: at higher currents like 1.6 MA, the stochastic loss threshold is larger and more difficult to exceed. The threshold at R = 2.6 m, I_P = 1.8 MA (Fig. 3f) is more similar to the R = 2.45 m, I_P = 1.6 MA case (Fig. 3d) than to the R = 2.6 m, I_P = 0.9 MA experiment (Fig. 3b), because the variation in q_a is so much stronger than the variation in major radius in these plasmas.

5.1.1. *Stochastic Diffusion Free Domains in RF Heated Plasmas*

Some initial projections for RF heated plasmas have been made, although full ORBIT calculations of loss fractions have not yet been carried out. For the TFTR experiments under consideration, the Larmor radius of a RF heated 700 keV He^3 minority ion is ≈ 2 cm. Figure 3g shows the stochastic ripple domain for such an ion at 1.8 MA and 2.6 m. Figures 3f and 3g show a reduced stochastic free region for alpha particles compared to the He^3 minority RF minority ions.

Figures 3f and 3g were used to interpret recent TFTR alpha charge exchange measurements, which had detected only He^3 signals during RF, but not alphas at the half radius [37, 38]. The alpha charge exchange measurements only see trapped ions in the plasma at a location illuminated by pellet injection. Since pellet injection has reached only to the half radius in the recent data, and pellet injection occurs after the beams are turned off, the alphas appear to have been lost by stochastic ripple diffusion, while RF ions remain in the larger stochastic ripple free region, and are observed with the diagnostic. Plans are being made for deeper pellet injection as well as for pellet injection during beam heating to study confined alpha particles. Parks [24] has developed an analytic model for the alpha distribution function expected with stochastic ripple diffusion.

5.2. *Neutral Beam Ion Diffusion*

Tables III and IV show predicted losses of the neutral beam ions for the two low current experiments simulated with ripple and collisional transport. In the tables 'Prompt' means losses occurring within twenty-five toroidal transits. For neutral beam ions this is within 150 μsec and for alpha particles this is within 35 μsec. The column in the tables labeled 'Prompt' is predominantly first orbit loss. Figures 4 and 5 show the evolution of the loss fractions for each beamline in the 0.9 MA and 1.0 MA experiments.

5.2.1. *Neutral Beam Ion Loss at 0.9 MA, 2.6 m*

Ripple and collisions along with first orbit losses cause a total loss of 38% of the fast ions during $\tau_\epsilon^{nb}/2$ for the 0.9 MA experiment. TRANSP calculations (which include collisions but not ripple) predict 8% neutral beam ions lost. From 38% ion losses we subtract the TRANSP calculated first orbit and collisional losses (8%) and multiply the result by the calculated beam fraction of β for these plasmas, $\beta^{nb}/\beta = 0.75$. The simulations predict ion losses which correspond to a reduction in plasma beta of 23%, close to the 28% beta discrepancy for I_P = 0.9 MA. Longer simulations (to τ_ϵ^{nb}) show small additional ripple losses $\leq 10\%$ at lower average energy, $\approx 0.45E_o$, which further improves agreement with measurements.

Table V shows the relative roles of ripple and collisions on the total prompt and delayed (non-first orbit) neutral beam losses for one counter-injected and one co-injected beamline from simulations of this experiment. The effect of collisions is not strong in increasing total losses compared to the 'Prompt' losses calculated neglecting collisions. Ripple alone is even less effective than collisions alone. Compared to the 'no ripple and no collisions' case, when collisions and ripple are added separately and then together, we see a strong synergistic enhancement of fast ion losses for both co-injected and counter-injected ions. The effect is not linear, in that the losses with collisions alone and with ripple alone cannot be simply added. In fact co-injected ion losses on TFTR are seen to be due entirely to the cooperative effect of ripple and collisions. As expected, there were no prompt losses for any co-injected neutral beam ions. Prompt losses are not affected by the presence of collisions or of ripple. A measure of the synergism is S, defined as the 'ripple and collisions' delayed loss divided by the sum of the delayed losses obtained with ripple alone and with collisions alone. We estimate S = (24/8 + 30/18)/2 = 2.3 for neutral beam ions on TFTR at 0.9 MA, averaging losses at R_T = -1.74 m and 1.80 m.

Figure 6 shows the poloidal distribution function for lost neutral beam ions at 0.9 MA at each beam injection angle. The poloidal distribution becomes broader and extends toward -90 degrees as R_T becomes more negative.

5.2.2. *Neutral Beam Ion Loss at 1.0 MA, 2.6 m*

For a similar experiment at I_P = 1.0 MA, with all co-injected ions, the simulations predict a 21% beam ion loss during $\tau_\epsilon^{nb}/2$ (Table IV). TRANSP calculates 3% first orbit and collisional losses and the beam ions contribute only 40% to beta for this case, so that the simulations account for a beta discrepancy of (21. - 3.)$\times$ 0.40 = 7%, close to the 8% discrepancy between measured and kinetically calculated beta.

5.2.3. Discussion of TFTR Neutral Beam Ion Loss

In Fig. 7 are shown orbits for an initially trapped neutral beam ion from the 0.9 MA case which is lost when ripple and collisions are included in the simulation to $\tau_\epsilon^{nb}/2$. The figure shows the 'no ripple and no collisions' case (7a), and the corresponding cases as ripple and collisions are turned on separately (7c, 7b) and together (7d), assuming the same initial ion parameters. In this figure each ion is followed up to 250 toroidal transits. Collisions affect counter-going neutral beam ion orbits more strongly than toroidal field ripple alone (Table V). In the figure. to show the effect of TF ripple on neutral beam ion orbits, pitch angle scattering rate was artificially enhanced toward more deeply trapped pitch angles. In Fig. 7b the ion pitch grows smaller with each collision, but the ion remains in the plasma; in Fig. 7d the combination of ripple and deeper trapping causes the ion to undergo stochastic diffusion and finally to become ripple trapped. In these figures the same pitch angle scattering algorithm is used in parts b and d of each figure. The accuracy of the Hamiltonian coordinate method is evident in the near perfect overlay of orbits for the simulation without ripple or collisions.

Our calculations were only carried out for full energy particles. To study differences in the transport of half and one third energy particles which each make up about 20% of the heating beams, simulations were done with half energy particles including increased pitch angle scattering (proportional to $1/\text{energy}^{3/2}$). It was found that particle losses decreased as energy decreased.

An additional source of fast particle losses might be due to δB from MHD activity. MHD was not present in any of the experiments discussed, above the level $\delta B/B = 10^{-3}$, which we have found is required for significant ion losses. We note that higher observed levels of MHD are correlated with a 38% beta discrepancy in a similar low current, large R TFTR experiment (shot 67255).

It is of interest to simulate the case of purely perpendicular injection for TFTR. Using the magnetic geometry of the 0.9 MA case with all beam lines injecting perpendicularly, the guiding center code simulations predict that 96% of the ions would be lost in $\tau_\epsilon^{nb}/2$, about half of which are prompt lost. This implies increased loss of fast ions for low current ICRH plasmas depending on the type of ICRF, the deposition profile and the minority ion energy.

The simulations indicate that most of the plasma energy missing from the low current experiments at 2.6 m was due to collisional stochastic ripple diffusion (CSRD) of fast beam ions not now included in the standard transport analysis. Additional anomalous fast ion diffusion processes were not required.

5.3. *Ripple Losses of Neutral Beam Ions on Other Large Tokamaks*

These results can be compared to neutral beam ripple losses reported for other large tokamaks. JET [18, 19, 25] observed ripple loss of beam and RF ions in experiments which compared 32 and 16 toroidal field coil discharges. Maximum ripple increased from 1% to 12.5% with this change in coil number. Reduction in coil number was found to correlate with a reduction of 30% in plasma stored energy. Only 10% of the neutral beam ions were expected to be first orbit lost in the 16 coil experiment. Recent analysis with the bounceaveraged RLX-1 Fokker Planck code [25] shows that 26% of the neutral beam ions are lost by the effects of ripple and collisional pitch angle scattering, with collisional stochastic losses due to change in ion toroidal angle, adding an additional 5%.

JT-60U [17] has large ripple losses because of large toroidal field ripple. Both parallel and near perpendicular neutral beam injectors may be used at JT-60U; with perpendicular injection a large fraction of the beam ions are trapped and subject to ripple losses. Tobita [17,26] has carried out studies of neutral beam ion losses for JT-60U with the Orbit Following Monte Carlo (OFMC) code, similar to the ORBIT code used here. Much of JT-60U's ripple losses are from ripple trapping, for which $\alpha^* = \epsilon|sin\theta|/(Nq\delta) < 1$. For both injection scenarios, calculations of the ripple loss fractions for JT-60U were found to be in good agreement with the experimental loss fractions.

Ions in TORE SUPRA [20], with perpendicular neutral beam injectors, are also strongly affected by ripple, because of the small number of toroidal field coils. In addition, the design of coils and vacuum vessel places the plasma close to the toroidal field coils, in the region of highest ripple. Experiments at TORE SUPRA were analysed with a model which predicted that 30% of neutral beam ions were lost, being directly generated in the stochastic ripple-loss domain.

Experiments at DIII-D [39], with near-tangential co-injected beams, did not find any indication of fast ion losses attributable to toroidal field ripple. DIII-D toroidal ripple is 1% at the plasma edge, half that of 2.6 m plasmas on TFTR. Experiments, with low ripple and for diverted, low Z_{eff} plasmas, would not be expected to show collisional enhancement of neutral beam ion stochastic ripple loss. As for JET also with small TF ripple and with near-tangential co-injected beams. collisionless stochastic ripple diffusion calculations are probably sufficient for transport analysis of experiments.

5.4. *Alpha Particle Diffusion*

The ORBIT guiding center code was also used to study the diffusion of a model alpha source profile, $(1-(r/a)^2)^9$. similar to a typical TRANSP calculated profile for a D and T beam simulation. Magnetic flux geometries from TFTR DD experiments at 2.45 m and 2.6 m were chosen as typical candidate TFTR DT experiments. In Tables VI–VIII are shown results for simulations with collisional (pitch angle scattering and energy slowing down) and ripple loss processes considered separately and together. Comparison of these guiding center code results to TRANSP, SNAP and MAPLOS analysis code calculations for the three experiments may be found in Ref. [40].

5.4.1. *Alpha Particle Loss at 0.9 MA, R = 2.6 m*

At $I_P = 0.9$ MA, R = 2.6 m ORBIT predicts that 34% of alphas would be lost after one energy slowing down time with 32% of the initial alpha source energy lost in this time (Table VI). The 'Prompt' losses are 21%. Note our definition of 'Prompt' (Sec. 5.2). High first orbit losses are predicted at 0.9 MA. The delayed losses are dominated strongly by ripple effects. Collisions are not important by themselves but only in concert with ripple diffusion, by collisional scattering of passing and trapped ions into the ripple loss domain. From Table

VI the synergistic effect of collisions is given by S = 13/9 = 1.4.

5.4.2. *Alpha Particle Loss at 1.8 MA, R = 2.6 m*

For the case at I_P = 1.8 MA, R = 2.6 m, with reduced q_a, the ORBIT predicted alpha loss fraction (23% particles, 19% energy) remains large (Table VII). This is a surprise, since the 'Prompt' losses at 1.8 MA are only 5-6% and the corresponding stochastic loss threshold map (Fig. 3f) does not imply high ripple losses for the very peaked alpha profile. In fact, the collisionless ripple loss is only 6%. The collisional losses by themselves are again unimportant, but the combination of ripple and collisions increases the alpha energy loss level from 12% to 19% so that from Table VII, S = 17/7 = 2.4.

5.4.3. *Alpha Particle Loss at 1.6 MA, R = 2.45 m*

Here again, as for neutral beam ions and the other alpha simulations, the individual roles of collisions and ripple are small (Table VIII). A synergistic enhancement when both processes are included causes the net loss across the plasma edge to be twice the 'Prompt' losses, if the limiter condition is set at the last closed flux surface. For R = 2.45 m we find 12% total particle losses when collisional losses are simulated and a synergistic effect, S = 12/8 = 1.5.

The previous ORBIT code simulations for the R = 2.45 m experiment lack one important feature - the plasma vacuum region between the plasma edge and the tokamak wall. This vacuum region is not significant for the R = 2.6 m cases which fill the vacuum vessel, but for the 2.45 m case, first orbit losses are overestimated since the last closed flux surface is used as the boundary for evaluating losses.

A last closed flux surface limiter condition defines particles as lost if they pass the last closed flux surface. In reality, some ions will continue on orbits partly outside the plasma, and remain to heat the plasma during part of their orbits. With vacuum region calculations, stochastic ripple losses are not expected to be reduced as much as first orbit losses are, since stochastic ripple diffusion rapidly moves the affected banana orbits outward toward the physical limiter.

Simulations of the 2.45 m case with the vacuum region included are 10-100 times more expensive in computer time than simulations with a limiter condition at the last closed flux surface, which required about 10 hours of cpu time on a Cray Y-MP C90. The time required is increased because this is a three-dimensional calculation, and in the vacuum region both q and δ are larger, leading to shorter time steps and longer total computation times. If the loss criterion is set to model a vacuum region rather than at the last closed flux surface, guiding center calculations yield about 5% first orbit losses. Rough extrapolated values in Table VIII assume that stochastic losses are unchanged when the vacuum region is included.

5.4.4. *Collision Modeling Sensitivity Study*

The above simulations used constant values of pitch angle scattering and slowing down rates. The effect of this approximation was studied by using other constant values as well as the radially dependent pitch angle scattering and drag rates calculated by the TRANSP code for the R = 2.6 m, I_P = 1.8 MA experiment (Table IX).

The radial variation of the rates was approximated by $\nu_{PA}(r) = 0.1/(1. + 2.5(r/a))$ and by $\nu_\epsilon(r) = 1.3/(1. - 0.87(r/a))$. These rates are normalized at the half radius to the constant values (0.039 sec^{-1}, 3.3 sec^{-1}) used for the simulations in Table VII. Simulations were also done with zero pitch angle scattering, halved pitch angle scattering (Z_{eff} reduced by a factor of 2), and doubled pitch angle scattering (*i.e.*, Z_{eff} increased by a factor 2). Simulations with radially varying rates and with doubled scattering predicted the same loss fractions within 2% as for the baseline simulations. Reducing Z_{eff} by a factor of two reduced the overall stochastic ripple diffusion losses by only about one-third. These results are not dependent on simulation particle number. Increased particle number (512 particles) did not change the loss fractions by more than 1% at the highest pitch angle scattering rate.

The change in delayed losses, $\Delta L_{delayed}(\nu_{PA}) = L_{delayed}(\nu_{PA}) - L_{delayed}(0)$ increases with ν_{PA}, but the change for $0.02 \text{ sec}^{-1} < \nu_{PA} < 0.078 \text{ sec}^{-1}$ is not large compared with the total delayed loss at $\nu_{PA} < 0.039 \text{ sec}^{-1}$. The collisional effects on stochastic ripple loss are seen to saturate near $\nu_{PA} = 0.078 \text{ sec}^{-1}$. The saturation in particle losses as Z_{eff} increases occurs because only particles near the boundary of the loss regions can be collisionally driven into the loss cone by pitch angle scattering during a slowing down time. It is helpful to refer here to Figs. 1, 11, 12 and 13. In the plasma simulations 26% of the alphas are initially trapped, 6% are first orbit lost and 6% are born with their bounce points in the stochastic loss region. As pitch angle scattering increases, the ion density adjacent to the stochastic region (see Fig. 1) will be depleted and continued increase in stochastic ripple losses will terminate. The detrapping effects of collisions will reduce SRD losses as the collision rate increases further until the loss rate is equal to the neoclassical diffusion rate. We estimate the neoclassical loss time to be 1000 seconds; the neoclassical loss rate is unimportant compared to the CSRD losses during τ_ϵ^α.

5.4.5. *Statistical Errors*

The Monte Carlo algorithm for the initial particle distribution leads to $\approx \pm\sqrt{N_{lost}}/N_{total}$ error in the loss fraction obtained. For the 2.6 m, 1.8 MA case and with a total 256 particles followed, for example, a 5% loss arising from 12 particles was predicted. The error in this calculation is $\sqrt{N_{lost}}/N_{total} = \pm 1.5\%$. The total particle loss, 23%, arose from 59 particles, so that the error in calculating the total loss is approximately $\sqrt{N_{lost}}/N_{total} = \pm 3\%$. As a check of these estimates, additional simulations with varied random number seed yielded a loss distribution in agreement with a spread limited by $\sqrt{2N}$, within which 2/3 of the Monte Carlo cases would be expected to occur.

5.4.6. *Summary Discussion of Alpha Losses*

Figure 8 shows individual alpha orbits for an initially trapped alpha particle, which is lost from the $I_P = 0.9$ MA, R = 2.6 m case when both ripple and collisional processes affect the orbit. The figure shows the no ripple and no collisions case as well as orbits which result from adding collisions and ripple separately and together. These simulations all assume the same initial alpha parameters and follow the ion for 250 toroidal transits. Figure 9 is an enlargement to show detail of Fig. 8c.

If we compare alpha particle orbits from Fig. 8 and neutral beam ion orbits which would correspond to Fig. 7 without artifically enhanced pitch angle scattering toward $\pi/2$, we find that ripple affects alpha particle orbits more strongly than collisions, in contrast to orbits of neutral beam ions. This can be understood as follows: Because the diffusion coefficient for stochastic ripple transport is that of ripple plateau, stochastic ripple diffusion is 150 times larger for alphas than for neutral beam ions. Since pitch angle scattering rates are inversely proportional to energy, the neutral beam ion pitch angle scattering rate is 100 times that of alphas in the same experiment (Table II), and the orbits of the less energetic neutral beam ions are more strongly affected by pitch angle scattering than are orbits of alpha particles.

Increased pitch angle scattering into the first orbit loss cone at low energies might have been expected to increase particle losses significantly. But, since adding collisions to the 'no ripple, no collisions' cases does not increase ion losses by more than a few percent, the reduction of the ion banana width by slowing down must nearly cancel the effect of the increased pitch angle scattering at low energies.

In Fig. 10 are shown the total losses calculated as a function of time for the three projected TFTR DT experiments. Note the suppressed zeroes; the prompt loss fractions are different for each case. The diffusive nature of the process is evident from the figure, with similar diffusion times at I_P/R = 0.9 MA/2.6 m and 1.8 MA/2.6 m. The relative rates of pitch angle scattering to slowing down for alphas are similar in all three cases (ν_{PA}/ν_ϵ = 0.007, 0.012, 0.011). The faster saturation for the 2.45 m plasma results from lower toroidal field ripple at small major radius and a proportionally larger stochastic free ripple domain (Fig. 3d).

Figures 11-13 show the initial ion parameters for alphas lost from the guiding center code simulations of the three projected DT TFTR experiments. μ is the inital ion magnetic moment; μ_o is the initial magnetic moment of an alpha born at the magnetic axis with $\pi/2$ pitch angle. Each ion lifetime (time to leave last closed flux surface of plasma) is indicated by a symbol with white diamonds and squares for first orbit loss events. Note that the first orbit loss and the stochastic ripple loss region-topologies are similar to Fig. 1. The first orbit loss region is much narrower for 1.8 and 1.6 MA (Figures 12, 13). Delayed loss events appear due to diffusion of passing particles into the prompt orbit loss cone from below as μ increases due to pitch angle scattering, when collisions are added to the no ripple and no collisions case. In all three figures these events occur only after alpha lifetimes greater than 2000 μsec (black squares). Delayed loss events representing diffusion of trapped particles from above into the ripple domain (due to reduction of μ by pitch angle scattering) and events due to collisionless stochastic ripple loss, are denoted by black diamonds and squares, for alpha lifetimes between 50 and 2000 μsec and greater than 2000 μsec. Most 'Prompt' losses are within the 10 microsecond time scale thought to characterize first orbit losses in fusion product measurements [12–14]. A statistically significant population characterized by time scales of 50-2000 μsec arises when ripple is added to the collisional simulations of the 0.9 MA case.

Figure 14 is a summary figure which combines results from high and low current ORBIT simulations at 2.6 m. The I_P dependence of first orbit losses, collisional losses, stochastic ripple diffusion (collisionless), and collisional stochastic ripple diffusion, as well as the total losses are shown. Collisional losses are small; first orbit losses decrease rapidly with increasing plasma current; stochastic ripple losses are $< 10\%$ but collisional stochastic ripple losses are $10-20\%$ and do not decrease as plasma current increases. They increase with plasma current for these simulations because the ratio of pitch angle scattering to slowing down increases with plasma current ($\nu_{PA}/\nu_\epsilon = .007$ at 0.9 MA, $\nu_{PA}/\nu_\epsilon = .012$ at 1.8 MA, Table II), and because the higher current experiment with high T_e had a longer alpha slowing down time. This caused increased collisional stochastic ripple diffusion for the higher I_P experiment. In general, higher plasma heating power can be used at increased plasma current, leading to higher electron temperatures so that increased CSRD is expected at high I_P. The synergistic enhancements are S = 1.4. 2.4. 1.5 for the alpha loss fractions of Tables VI–VIII.

5.4.7. Comparison with Experiment

Initial analyses of 1993-1994 TFTR DT experiments by Janos [41] for wall heating and by Darrow [42] for alpha loss do not require alpha loss rates greater than 20-30%, as predicted by these simulations.

Zweben [43] has observed a delayed loss of DD fusion products at 90 degrees below the plasma midplane in R = 2.45 m plasmas, but not in 2.62 m plasmas. It is interesting to see what our simulations predict for the poloidal and pitch angle distributions of fast particle losses. Figures 15 and 16 show the predicted final poloidal and pitch angle distributions of 'Prompt' and total loss fractions for alpha particles as calculated for the TFTR experiments at 0.9 MA and 1.8 MA for R = 2.6 m. The figures show the fractions lost as a function of poloidal angle in units of radians and as a function of the cosine of the pitch angle.

Figure 15 shows losses peaked just below the midplane in all cases with the prompt loss events being much less strongly peaked about the midplane than the total of prompt and stochastic losses. The low current case shows a greater likelihood of events at 90 degrees than the 1.8 MA case. Some alpha loss events are predicted near the 90 degree detector location, while simulations of neutral beam ions (Fig. 6) lead to no events at 90 degrees for either current. ORBIT's ratios of alpha loss events at 20±5 degrees to those seen at 45±5 degrees are as follows: $R_{loss} = 4/3$ for 0.9 MA and $R_{loss} = 11/2$ at 1.8 MA, while less variation (3/2) is seen in comparing 0.9 MA to 1.8 MA at 45 degrees. With a window of ±10 degrees at 45 degrees the ratio of lost alphas at 0.9 MA to those at 1.8 MA is 3/6, reflecting the increased stochastic loss rate at high current.

What do these time dependent results suggest concerning the delayed losses observed by Zweben [43] at 2.45 m but not at 2.62 m? The long time scale is compatible with the simulations of *collisional* stochastic ripple diffusion. Although most stochastic losses do take place quickly after the birth of the particle, there will always be some losses later in the ion's lifetime, as the eventual effect of pitch angle scattering plus ripple deformation of field lines and ion orbits accummulates (Fig. 10). More fusion products from plasmas at 2.62 m are born in regions of strong ripple than at 2.45 m and a greater fraction are quickly lost through collisionless stochastic ripple diffusion. At 2.45 m, more fusion products not immediately lost to stochastic ripple diffusion are available to be collisionally driven into the stochastic loss region and the first orbit loss cone during the ions' slowing down time.

5.5. *Control of Stochastic Ripple Loss*

How can these collisional stochastic ripple losses be controlled in a tokamak with nonzero edge ripple? The simulation results showed that the diffusive effect of stochastic ripple losses on fast ions is greatly enhanced by the presence of collisions. The resulting losses can be reduced by shortening the energy slowing time so that pitch angle scattering losses do not accumulate, by reducing the pitch angle scattering rate or by increasing the size of the stochastic free region by reducing the ripple strength.

Standard formula for collision rates lead to

$$\tau_\epsilon^{nb/i'} \sim 1/n_e,$$

$$\tau_\epsilon^{\alpha/e} \sim T_e^{3/2}/n_e$$

and

$$\nu_\perp^{nb/i'}, \nu_\perp^{\alpha/i'} \sim n_{i'} Z_{i'}^2 \sim n_e Z_{eff}.$$

Pitch angle scattering can be reduced for both neutral beam and alpha particles in plasmas if Z_{eff} is lowered. Operating at lower T_e, as in pellet experiments, will shorten $\tau_\epsilon^{\alpha/e}$. $\tau_\epsilon^{\alpha/e}$ and $\tau_\epsilon^{nb/i'}$ will be reduced for experiments at higher n_e. But since $\nu_\perp$ is also proportional to n_e, control of ripple losses would require tuning the density to find the optimal value for reduced pitch angle scattering and shortened slowing down time.

A method for burn control for fusion reactor operation may be achievable through this collisional control of stochastic ripple diffusion. Impurity puffing or injection at the plasma edge could be applied to vary Z_{eff}, T_e, *etc.* during reactor operation. Care would be needed not to trigger quenching of ignition or disruption, and to prevent excessive localized wall heating. From Table IX we can estimate a quantitative measure of this control: Halving Z_{eff} (3 to 1.5) and reducing ν_{PA} from 0.039 to .020 sec^{-1}, ripple loss heat loading of the first wall/limiter is reduced by about 50%. Doubling Z_{eff} (from 3 to 6) and increasing ν_{PA} from 0.039 to 0.078 sec^{-1} has a much smaller effect, increasing the heat load by about 10%.

Fisch [44] has recently suggested that RF could be used to rapidly catalyze direct conversion of alpha particle energy into the energy of D and T reactor fuel ions. If the catalysis is rapid and efficient enough (within 25–50 μsec) non-first orbit alpha particle energy can be utilized for fusion before stochastic ripple losses occur.

6. Toroidal Field Error Induced Fast Ion Losses

The actual vacuum TFTR field has been measured leading to a model for field errors due to radial displacements of -1.0, -2.0, -2.0, 1.8, 1.8 cm for TFTR coils 2–6 (Fig. 17). (A rotation of .04 degrees for the fourth coil was also found.) This is about the same size as the toroidal field ripple at the plasma center. At R = 2.95 m, the toroidal field ripple is 0.0006, and the toroidal field error is 0.0005. With an effective coil number of 3, rather than 20, δ_s is increased by a factor of 17. Consequently the stochastic criterion is not likely to be exceeded by the field error, in the outer half of the plasma where ripple is dominated by the discreteness of the coils. Toroidal field errors are not expected to cause significant fast ion losses for most experiments at TFTR.

Johnson and Reiman [45] have looked into the effect of plasma currents interacting with the plasma ripple at finite beta and find that the dominant effect comes from the Shafranov shift of the magnetic axis so that a greater fraction of the plasma is in the ripple domain. This effect has been included in our work. Other intrinsic plasma response to the ripple field is not expected to be large.

7. Conclusion

Monte Carlo Hamiltonian coordinate-following code simulations of two low current TFTR experiments predict that 38% and 21% of the injected neutral beam ions were lost due to 'Prompt' and collisional stochastic ripple diffusion over $\tau_\epsilon^{nb}/2$ and thus resolve kinetic transport analysis discrepancies of 28% and 8% with measured beta. Additional anomalous fast ion transport was not found necessary for neutral beam ions for these plasmas. The poor performance of large major radius, high q_a supershots appears to be due in part to these prompt and collisional stochastic ripple losses.

A synergistic enhancement for ripple with collisions was found to increase the total losses for neutral beam ions and alpha particles. 20% losses of alpha particles and alpha heating are projected for DT experiments on TFTR at 2.6 m for 1.8 MA plasmas, with higher losses at lower current. Toroidal field error induced fast ion losses, due to imperfectly aligned coils, are expected to be small on TFTR.

The guiding center code simulations showed enhanced fast ion losses with ripple and collisions acting together. This synergism arises because pitch angle scattering allows ions to be scattered into *both* the first orbit loss and the stochastic loss regions, when TF ripple opens the stochastic loss region. The effect is also large because losses are accumulated over the ion slowing down time. Consideration of scattering rates suggests that operating at low Z_{eff} will keep ripple diffusion losses low by reducing pitch angle scattering and that alpha loss can be minimized by operating at lower T_e to shorten slowing down times. Alpha losses will be minimized if I_P is large and R is small, as for most TFTR DT experiments. However, discharges at large R to study RF heating and current drive and discharges at low current, will be subject to stronger ripple diffusion so that control of these losses by operating at reduced Z_{eff}, T_e is even more desirable. Experimentally validated computer simulations of fast ion collisional stochastic ripple diffusion are needed for the design of future fusion devices like TPX [46], SSTR [47], and ITER [48], for which ripple losses of alphas are now a central issue.

Acknowledgment

The authors would like to acknowledge useful discussions with R. Boivin, C. S. Chang, E. Fredrickson, S. Medley. Assistance by M. Manickam with the PEST code and by M. Chance with the MAPPING code is gratefully acknowledged. PPPL research students A. Smitten and A. Marks contributed excellent computational support. We are glad to thank R. Goldston, R. Hawryluk and K. McGuire for their interest. This work was supported by the U. S. Department of Energy Contract No. DE-AC02-76-CHO-3073.

References

[1] Yushmanov, P. N., Nucl. Fusion **23** (1983) 1599.

[2] Yushmanov, P. N., *et al.*, Nucl. Fusion **33** (1993) 1293.

[3] Chang, C. S. and Zweben. S. J., "Model for Collisional Fast Ion Diffusion into the TFTR Loss Cone" Collisional Loss of Energetic Ions into a Tokamak First Orbit Loss Cone" PPPL-3005(1994), Physics of Plasmas, in press (1994).

[4] Boozer, A. H., Phys. Fluids **23** (1980) 2283.

[5] Goldston, R. J., *et al.*, Phys. Rev. Lett. **47** (1981) 647.

[6] Shasharina, S. G. and Cary, J. R., Nucl. Fusion **33** (1993) 648.

[7] White, R. B. and Chance, M. S., Phys. Fluids **27** (1984) 2455.

[8] White, R. B., Phys. Fluids **B2** (1990) 845.

[9] White, R. B., Theory of Tokamak Plasmas, North Holland Pub. Co., 1989, Amsterdam, 361 pp.

[10] Goldston, R. J. and Towner, H. H., J. Plasma Phys. **26** (1981) 283.

[11] Scott, S. D., *et al.*, Nucl. Fusion **25** (1985) 359.

[12] Boivin, R. L., *et al.*, Nucl. Fusion **33** (1993) 449.

[13] Zweben, S. J., *et al.* IAEA conference, **1** (1992) 363, Wurzburg, Germany.

[14] Budny, R. V., Nucl. Fusion **34** (1994) 1247.

[15] White, R. B. and Mynick, H. E., Phys. Fluids **B1** (1989) 980.

[16] Zweben, S. J., *et al.*, Nucl. Fusion **31** (1991) 2219. Sept (1993) 61pp.

[17] Tobita, K.,*et al.*, Phys. Rev. Lett. **69** (1992) 3060–3063.

[18] Sadler, G., *et al.*, in *Proceedings of the 1992 International Conference on Plasma Phys., Innsbruck* (European Physical Society, Petit-Lancy, Switzerland, 1992), Vol. 1, p. 167.

[19] Tubbing, B., *et al.* 14th IAEA Conf. On Plasma Phys. and Controlled Fusion Research, Wurzburg, 1992.

[20] Basiuk, V. *et al.*, in *Proceedings of the 1992 International Conference on Plasma Phys., Innsbruck* (European Physical Society, Petit-Lancy, Switzerland, 1992), Vol. 1, p. 175.

[21] Tani, K., *et al.*, Nucl. Fusion **33** (1993) 903-914.

[22] Tani K., *et al.*, J. Phys. Soc. Japan **50** (1981) 1726-1737.

[23] Tani, K., *et al.*, Nucl. Fusion **23** (1983) 657-665.

[24] Parks, P. B, *et al.*, "Effect of Stochastic Ripple Diffusion on the Detection of Fusion Product Ions by Charge Exchange Pellet Diagnostics", Nucl. Fusion in press.

[25] Putvinskij, S. V., *et al.*, Nucl. Fusion **34** (1994) 495.

[26] Tobita, K., *et al.*, Nucl. Fusion, **34** 8 (1994) 1097.

[27] Eriksson, L.-G. and Helander, P., Nucl. Fusion, **33** (1994) 767.

[28] Towner, H. H. *et al.*, Rev. Sci. Instrum. **6** (1992) 4753.

[29] Hawryluk, R., *et al.*. Proceedings of the Course on Physics of Plasmas Close to Thermonuclear Conditions (Commission of the European Communities, Brussels, 1980) Report EUR FU, BRU/XII/476/80 Vol. 1, p 19 ; Goldston, R. J., *et al.*, J. Comput. Phys. **43** 61 (1981).

[30] Batistioni, P. and Barnes, C. W., Plasma Phys. Controlled Fusion **33** (1991) 1735.

[31] Book, David L., NRL Plasma Formulary, Washington, D. C., NRL Publication 177-4405, (1990) 64pp.

[32] Grimm, R. C., *et al.*, Meth. Computing Physics **9** (1974) 253.

[33] Grimm, R. C., *et al.*, J. Comput. Phys. **49** (1983) 94-117.

[34] Budny, R. V., *et al.*, Nucl. Fusion **32** (1992) 429-447.

[35] Hawryluk, R., *et al.* Phys. Rev. Lett., **72** (1994)3530.

[36] Strachan, J. D., *et al.*, Phys. Rev. Lett., **72** (1994) 3526.

[37] McChesney, J. M., *et al.* Rev. Sci. Instrum. **66**, 1, (1995) 348.

[38] Medley, S. S., *et al.*. Proceedings of the Twentieth European Physical Society Conference on Controlled Fusion and Plasma Phys. (Lisbon, Portugal, July 1993) Vol. III 1183-1186.

[39] Duong, H. H. and Heidbrink, W. W., Nucl. Fusion **33** (1993) 211-224.

[40] Redi, M. H., *et al.*, "Collisional Stochastic Ripple Diffusion of Alpha Particles and Beam Ions on TFTR", PPPL-3011, Princeton Plasma Physics Laboratory Report, Princeton University, Princeton. N. J., September, 1994, 61pp.

[41] Janos, A. C., *et al.* Rev. Sci. Instrum. **66**, 1, (1995) 354.

[42] Darrow, D., *et al.* Rev. Sci. Instrum. **66**, 1, (1995) 476.

[43] Zweben, S. J., *et al.*, Nucl. Fusion **33** (1993) 705-724.

[44] Fisch, N. and Rax, J-M, Phys. Rev. Lett. **69** (1992) 612;. Fisch, N., *et al.*, Plasma Phys. Controlled Fusion (IAEA 92) (1993) 769; Fisch, N., Phys. Fluids **B** 5, (1993) 1754.

[45] Johnson, J. L., Reiman, A. H., Nucl. Fusion **28** (1988) 1116–1120.

[46] Schmidt, J. A., *et al.*, J. Fusion Energy, **12** (1993) 455.

[47] Kikuchi, M., Nucl. Fusion **30** (1990) 265-276.

[48] Shimomura, Y., *et al.* Overview of the International Thermonuclear Experimental Reactor, Physics of Plasmas, 1 (1994) 1610-1616.

Table I. TFTR Experiments Simulated

Shot	R (m)	a (m)	B_T (T)	I_P (MA)	q_a	P_{inj} (MW)	E_{nb} (keV)	$\Delta\beta$ (%)
67241	2.6	.96	4.5	0.9	14.	13.	95.	28.
67243	2.6	.96	4.5	1.0	11.	9.	95.	8.
67885	2.6	.96	4.8	1.8	6.	23.	101.	–
55851	2.45	.80	5.1	1.6	5.6	25.	105.	–

Table II. Simulation Parameters

shot	67241	67243	67885	55851
$\nu_{pa}^{nb}(sec^{-1})$	2.5	.77	–	–
$\nu_{pa}^{\alpha}(sec^{-1})$	.030	–	.039	.047
$\tau_{\epsilon}^{nb}(sec)$	.34	.73	–	–
$\tau_{\epsilon}^{\alpha}(sec)$	.23	–	.30	.23
$n_{eo}(10^{13}/cm^3)$	3.8	2.	5.2	8.5
$T_{eo}(keV)$	6.0	6.5	9.0	10.5
$< n_e > (10^{13}/cm^3)$	2.	1.	2.5	3.5
$< T_e > (keV)$	3.5	3.5	2.5	6.0
Z_{eff}	3.2	2.	3.3	2.9
$\tau_{tran}^{d}(\mu s)$	6.1	5.9	–	–
$\tau_{tran}^{\alpha}(\mu s)$	1.4	–	1.4	1.3

Table III. Fraction of Neutral Beam Ions Lost in Simulations of TFTR High q_a Experiment 67241 during $\tau_\epsilon^{nb}/2$

R_T (m)	Fraction Lost (%)		
	Prompt	Delayed	Total
-2.23	30.	17.	47.
-1.99	38.	15.	53.
-1.74	35.	24.	59.
1.80	1.	29.	30.
1.99	0.	24.	24.
2.29	0.	19.	19.
average	17.	21.	38.

Table IV. Fraction of Neutral Beam Ions Lost in Simulations of TFTR High q_a Experiment 67243 during $\tau_\epsilon^{nb}/2$

R_T (m)	Fraction Lost (%)		
	Prompt	Delayed	Total
1.80	0.	30.	30.
1.99	0.	26.	26.
2.05	0.	19.	19.
2.29	0.	10.	10.
average	0.	21.	21.

Table V. Effect of Ripple and Collisions on Prompt

and Delayed Neutral Beam Losses (%)

for I_P = 0.9 MA, R = 2.6 m (67241) during $\tau_\epsilon^{nb}/2$

Col	Rip	R_T (m)	Prompt	Delayed	Total
–	–	-1.74	35.	0.	35.
√	–	-1.74	35.	6.	41.
-	√	-1.74	35.	2.	37.
√	√	-1.74	35.	24.	59.
–	–	1.80	0.	0.	0.
√	–	1.80	0.	8.	8.
–	√	1.80	0.	10.	10.
√	√	1.80	1.	30.	31.

Table VI. Alpha Losses (%) during τ_ϵ^α for I_P =0.9 MA. R = 2.6 m (67241)

Collisions	Ripple	Prompt	Delayed	Total	Energy
–	–	21.	0.	21.	21.
√	–	21.	2.	23.	23.
–	√	22.	7.	29.	29.
√	√	21.	13.	34.	32.

Table VII. Alpha Losses (%) during τ_ϵ^α for I_P = 1.8 MA, R = 2.6 m (67885)

Collisions	Ripple	Prompt	Delayed	Total	Energy
–	–	5.	1.	6.	6.
√	–	5.	1.	6.	6.
–	√	6.	6.	12.	12.
√	√	6.	17.	23.	19.

Table VIII. Alpha Losses (%) during τ_ϵ^α for I_P = 1.6 MA, R = 2.45 m (55851)

Collisions	Ripple	Prompt	Delayed	Total	Energy
Last Closed Flux Surface Limiter					
–	–	9.	0.	9.	9.
√	–	9.	3.	12.	11.
–	√	9.	5.	14.	14.
√	√	9.	12.	21.	20.
Experimental Limiter Location:					
√	√	5.5	12.[a]	17.5[a]	16.5[a]

[a]Extrapolation

Table IX. Alpha Losses (%) during τ_ϵ^α for I_P = 1.8 MA, R = 2.6 m (67885) with Variations in Collision Modeling

ν_{PA} (sec^{-1})	ν_ϵ (sec^{-1})	Prompt (%)	Delayed (%)	Total (%)
0.	0.	6.	7.	13.
0.	3.3	6.	5.	11.
.020	3.3	6.	11.	17.
.039	3.3	6.	17.	23.
$\nu_{PA}(r)$	$\nu_\epsilon(r)$	6.	16.	22.
.078	3.3	6.	19.	25.
.078	3.3	7.[a]	18.[a]	25.[a]

[a]512 particles

Figures

Fig. 1. Topology of trapped and passing ions and the first orbit and stochastic ripple loss domains plotted as a function of initial magnetic moment and outer midplane crossing point. This sketch is approximately correct only for very high energy particles. The loss region extends to $r/a \approx 0.2$, with significant trapped particles confined on axis.

Fig. 2. TFTR ripple contours; bold line denotes the vacuum vessel.

Fig. 3. TFTR stochastic ripple loss criteria δ/δ_s for fast beam ions and alpha particles for I_P/R = 0.9 MA/2.6 m (a, b); and for 1.6 MA/2.45 m (c, d); for fast beam ions, alpha particles and RF heated He^3 ions for 1.8 MA/2.6 m (e, f, g).

Fig. 4. Evolution of loss fractions for neutral beam ions over $\tau_\epsilon^{nb}/2$ for 0.9 MA, R = 2.6 m with R_T = a) -2.23 m, b) -1.99 m, c) -1.74 m, d) 1.80 m, e) 1.99 m, and f) 2.29 m.

Fig. 5. Evolution of loss fractions for neutral beam ions over $\tau_\epsilon^{nb}/2$ for 1.0 MA, R = 2.6 m with R_T = a) 1.80 m, b) 1.99 m, c) 2.05 m, and d) 2.29 m.

Fig. 6. Poloidal distributions of neutral beam ion loss fractions over $\tau_\epsilon^{nb}/2$ at 0.9 MA, 2.6 m for R_T = a) -2.23 m, b) -1.99 m, c) -1.74 m, d) 1.80 m, e) 1.99 m, and f) 2.29 m for poloidal angle in units of radians.

Fig. 7. Individual neutral beam ion orbits for the 0.9 MA experiment with a) ripple and collisions off; b) ripple off, collisions on; c) ripple on, collisions off; and d) ripple and collisions on.

Fig. 8. Individual alpha particle orbits for the 0.9 MA experiment with a) ripple and collisions off; b) ripple off, collisions on; c) ripple on, collisions off; and d) ripple and collisions on.

Fig. 9. Enlargement of individual alpha particle orbits for the 0.9 MA experiment with ripple on, collisions off.

Fig. 10. Evolution of total loss fractions of alphas from simulations of TFTR experiments at a) R = 2.6 m, I_P = 0.9 MA; b) R = 2.6 m, I_P = 1.8 MA; and c) R = 2.45 m, I_P = 1.6 MA.

Fig. 11. Initial magnetic moments and plasma radii (in units of poloidal magnetic flux, Ψ, normalized by Ψ at the plasma edge) of lost alphas for I_P = 0.9 MA, R = 2.6 m with ripple and collisions as a function of ion's lifetime within the plasma.

Fig. 12. Initial magnetic moments and plasma radii (in units of poloidal magnetic flux, Ψ, normalized by Ψ at the plasma edge) of lost alphas for I_P = 1.8 MA, R = 2.6 m with ripple and collisions as a function of ion's lifetime within the plasma.

Fig. 13. Initial magnetic moments and plasma radii (in units of poloidal magnetic flux, Ψ, normalized by Ψ at the plasma edge) of lost alphas for I_P = 1.6 MA, R = 2.45 m with ripple and collisions as a function of ion's lifetime within the plasma.

Fig. 14. I_P dependence of alpha loss fractions at 2.6 m, showing first orbit, collisional, stochastic ripple diffusion, collisional stochastic ripple diffusion and total loss fractions.

Fig. 15. Poloidal distributions of alpha particles: 'Prompt' loss events from simulations of a) the 0.9 MA experiment and b) the 1.8 MA experiment; total loss events from c) the 0.9 MA experiment and d) the 1.8 MA experiment. Poloidal angle in units of radians.

Fig. 16. Pitch angle distributions of alpha particles: 'Prompt' loss events from simulations of a) the 0.9 MA experiment and b) the 1.8 MA experiment; total loss events from c) the 0.9 MA experiment and d) the 1.8 MA experiment.

Fig. 17. Toroidal field error at R = 2.95 m on TFTR.

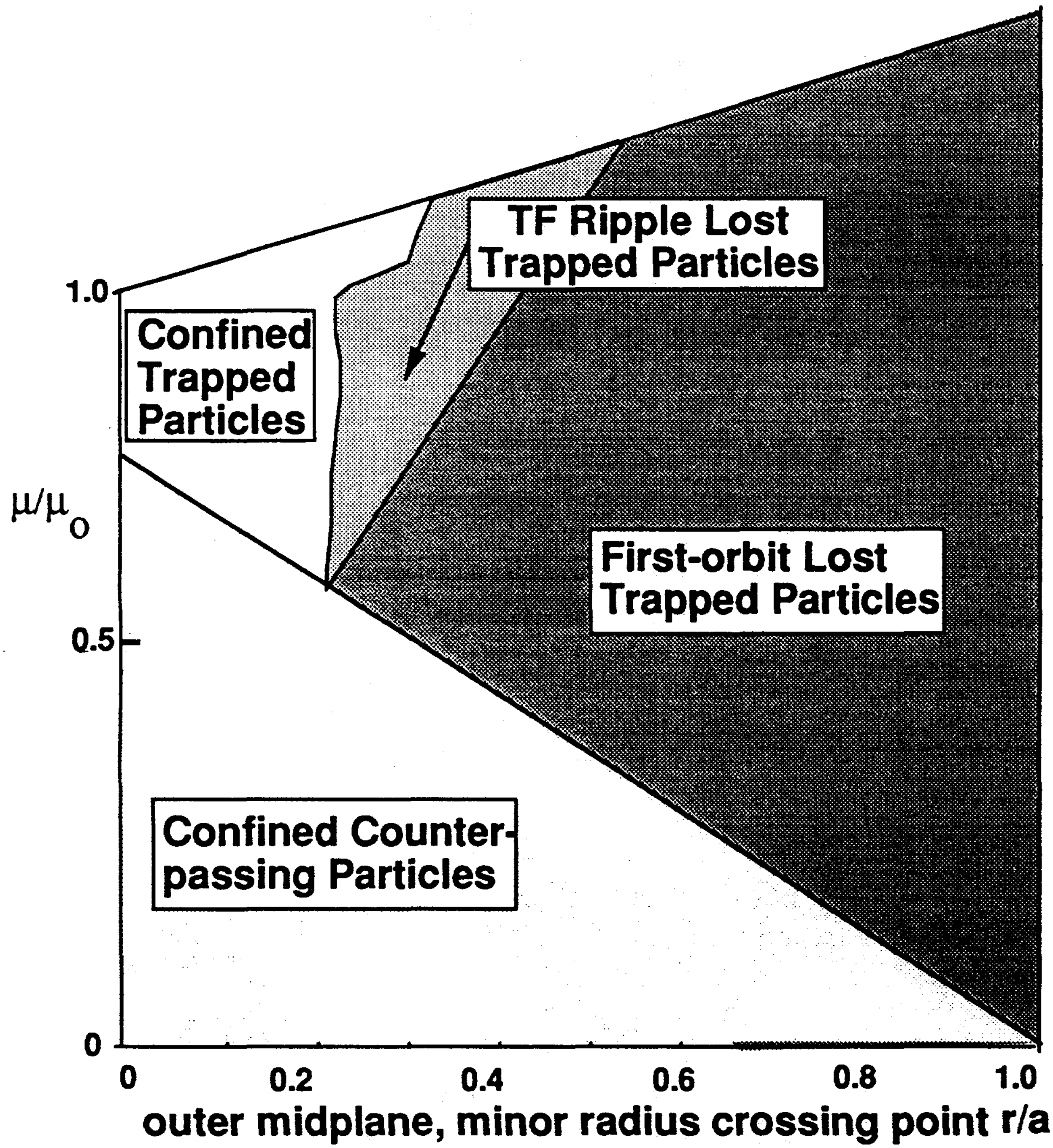
TF Ripple Lost
Trapped Particles
Confined
Trapped
Particles
First-orbit Lost
Trapped Particles
Confined Counter-
passing Particles
μ/μo
1.0
0.5
0
0
0.2
0.4
0.6
0.8
1.0
outer midplane, minor radius crossing point r/a

Fig. 1

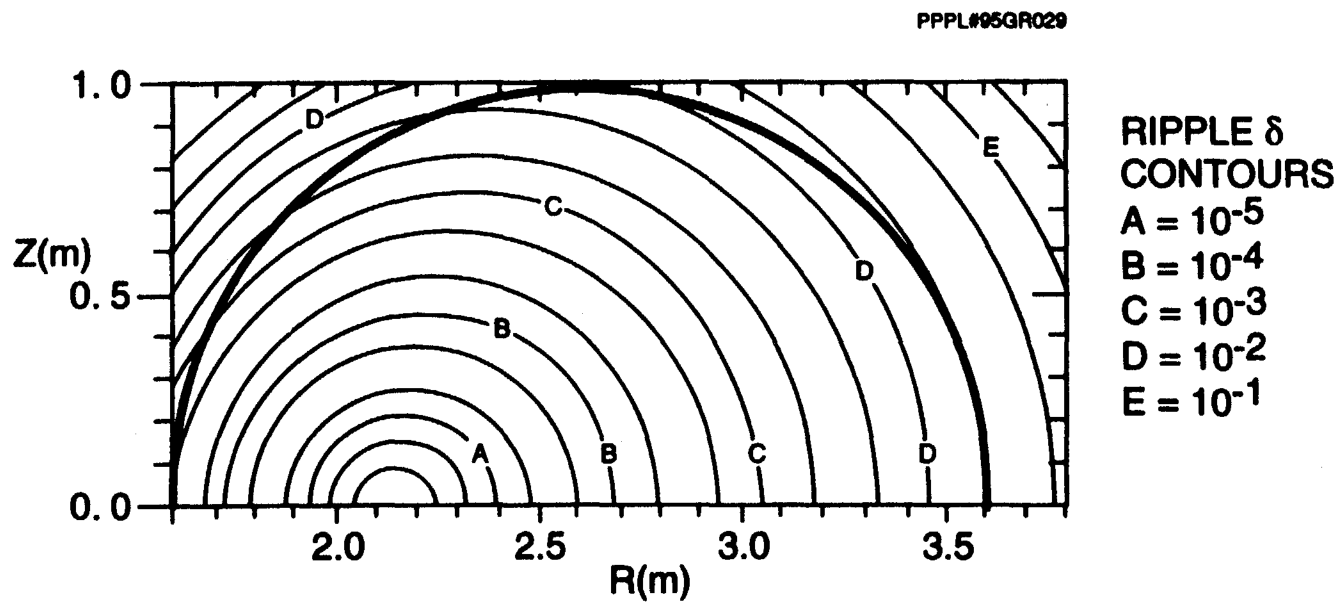
PPPL#95GR029
Z(m)
1.0
0.5
0.0
R(m)
2.0
2.5
3.0
3.5
A
B
C
D
E
RIPPLE δ
CONTOURS
A = 10^{-5}
B = 10^{-4}
C = 10^{-3}
D = 10^{-2}
E = 10^{-1}

Fig. 2

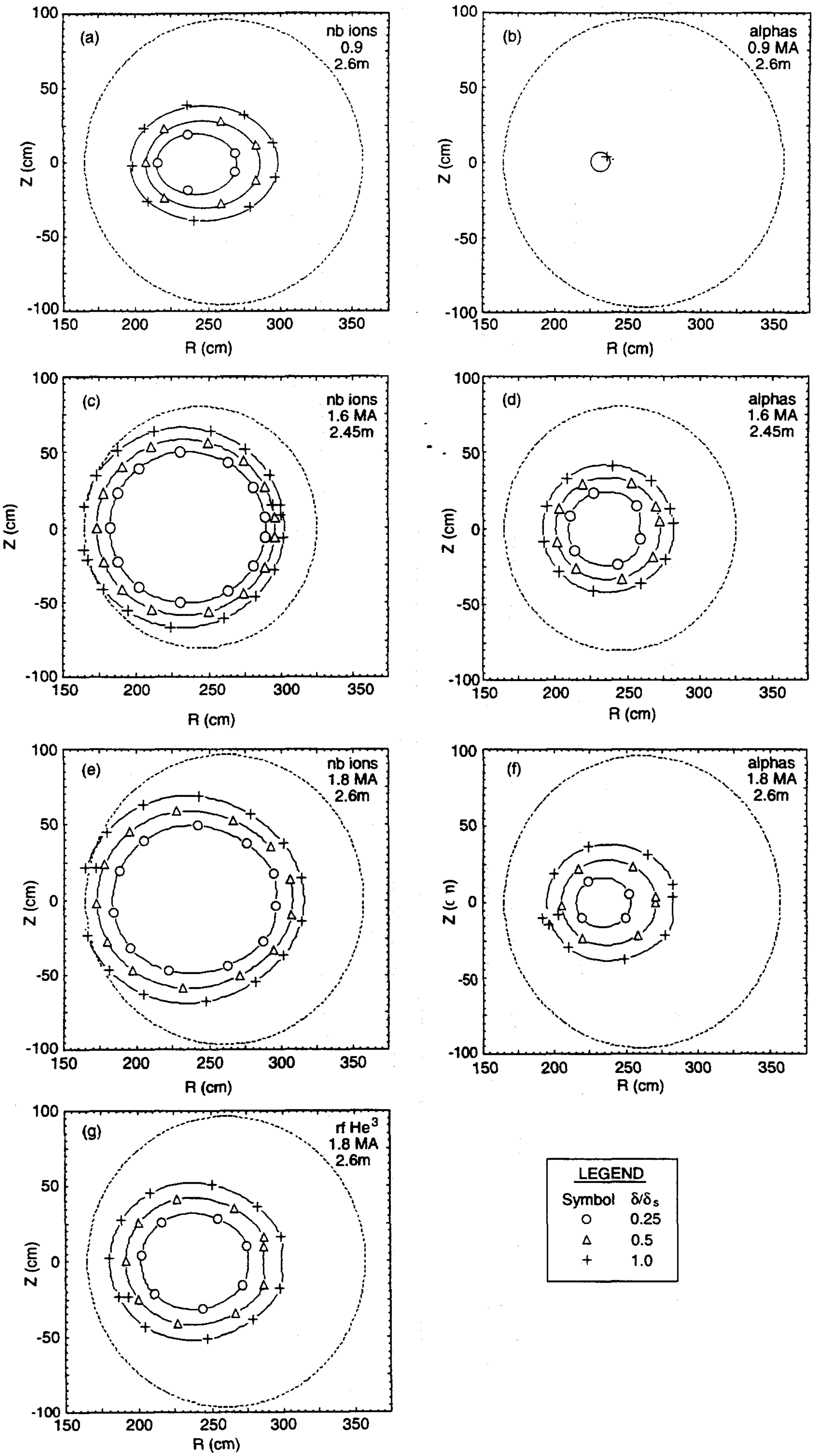
(a)
nb ions
0.9
2.6m
(b)
alphas
0.9 MA
2.6m
(c)
nb ions
1.6 MA
2.45m
(d)
alphas
1.6 MA
2.45m
(e)
nb ions
1.8 MA
2.6m
(f)
alphas
1.8 MA
2.6m
(g)
rf He3
1.8 MA
2.6m
Z (cm)
R (cm)
LEGEND
Symbol δ/δs
○ 0.25
△ 0.5
+ 1.0

Fig. 3

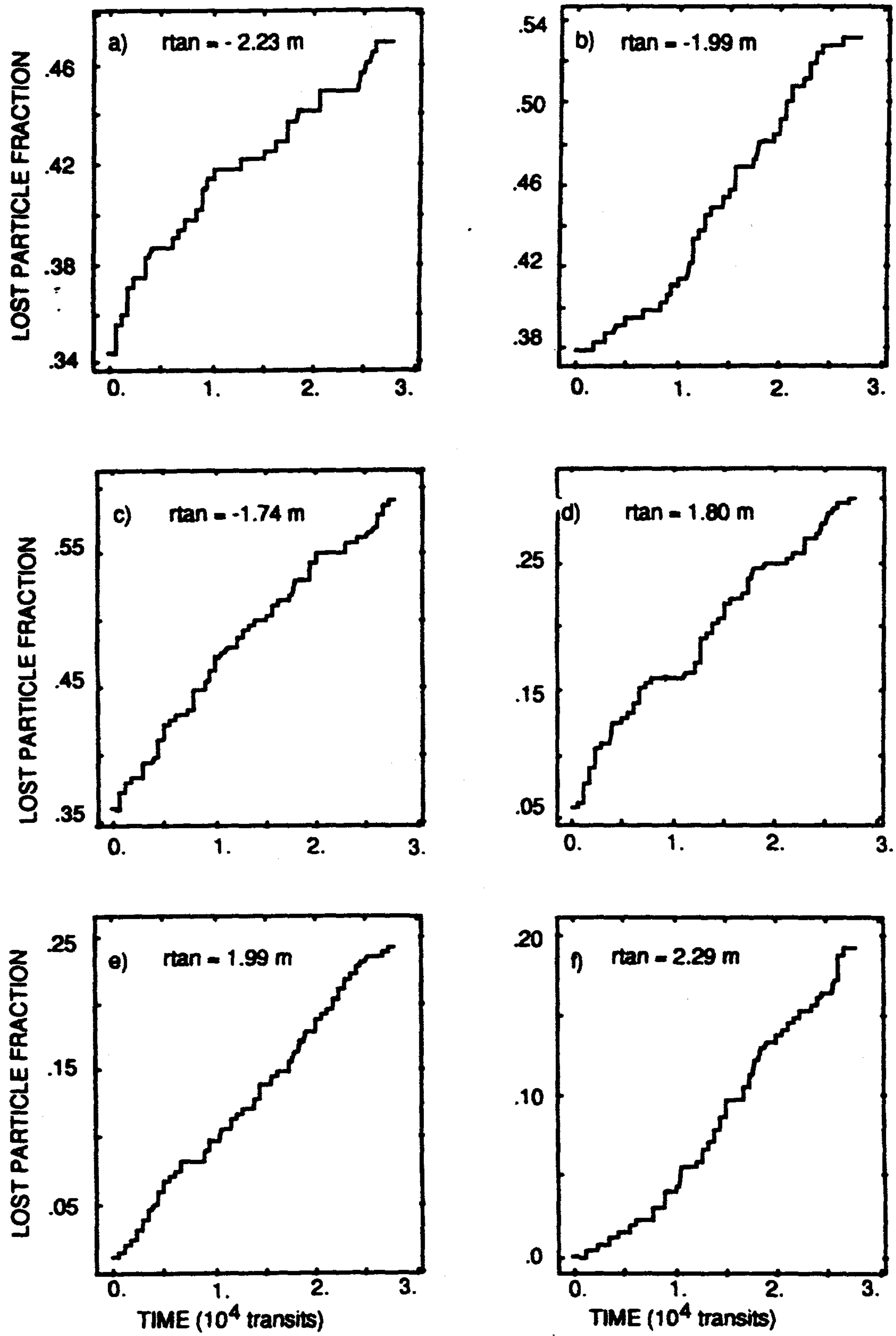

a) rtan = - 2.23 m
b) rtan = -1.99 m
c) rtan = -1.74 m
d) rtan = 1.80 m
e) rtan = 1.99 m
f) rtan = 2.29 m
LOST PARTICLE FRACTION
.34
.38
.42
.46
.38
.42
.46
.50
.54
.35
.45
.55
.05
.15
.25
.05
.15
.25
.0
.10
.20
0.
1.
2.
3.
TIME (10^4 transits)

Fig. 4

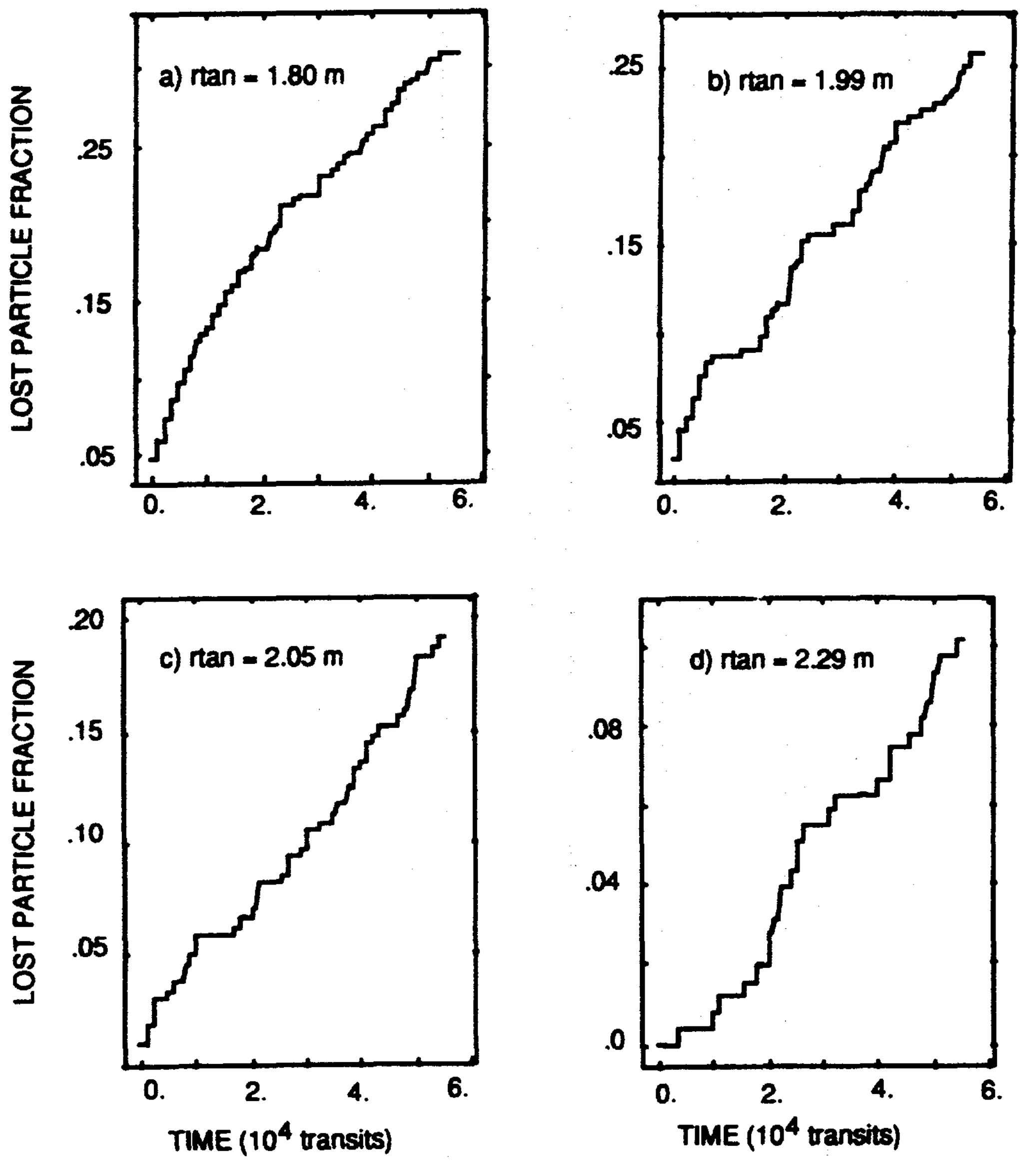

a) rtan = 1.80 m
b) rtan = 1.99 m
c) rtan = 2.05 m
d) rtan = 2.29 m
LOST PARTICLE FRACTION
LOST PARTICLE FRACTION
.05
.15
.25
.05
.15
.25
.20
.15
.10
.05
.08
.04
.0
0.
2.
4.
6.
TIME (10^4 transits)
TIME (10^4 transits)

Fig. 5

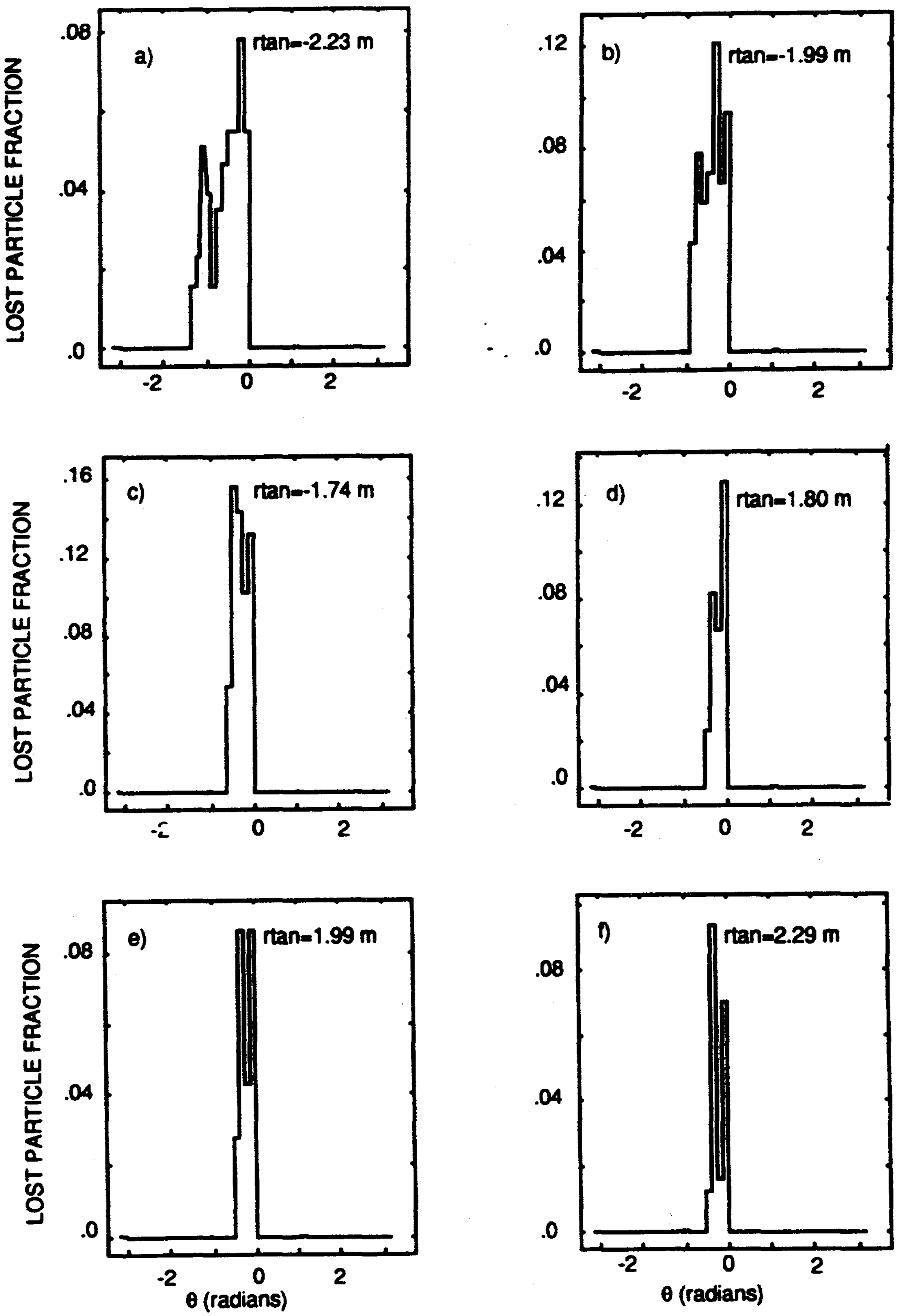
a)
rtan=-2.23 m
b)
rtan=-1.99 m
c)
rtan=-1.74 m
d)
rtan=1.80 m
e)
rtan=1.99 m
f)
rtan=2.29 m
LOST PARTICLE FRACTION
θ (radians)

Fig. 6

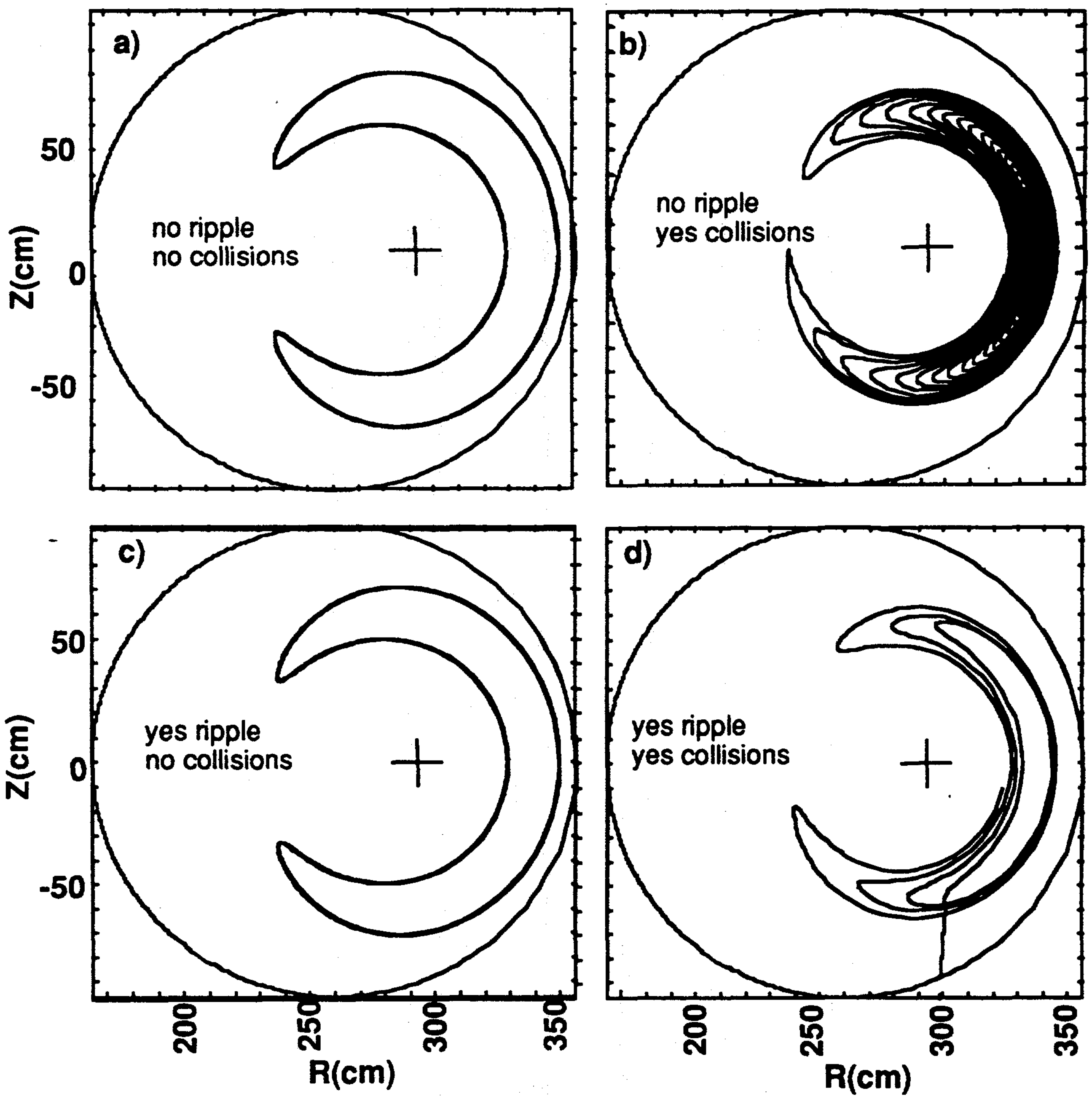

a)
no ripple
no collisions
b)
no ripple
yes collisions
c)
yes ripple
no collisions
d)
yes ripple
yes collisions
Z(cm)
50
0
-50
R(cm)
200
250
300
350

Fig. 7

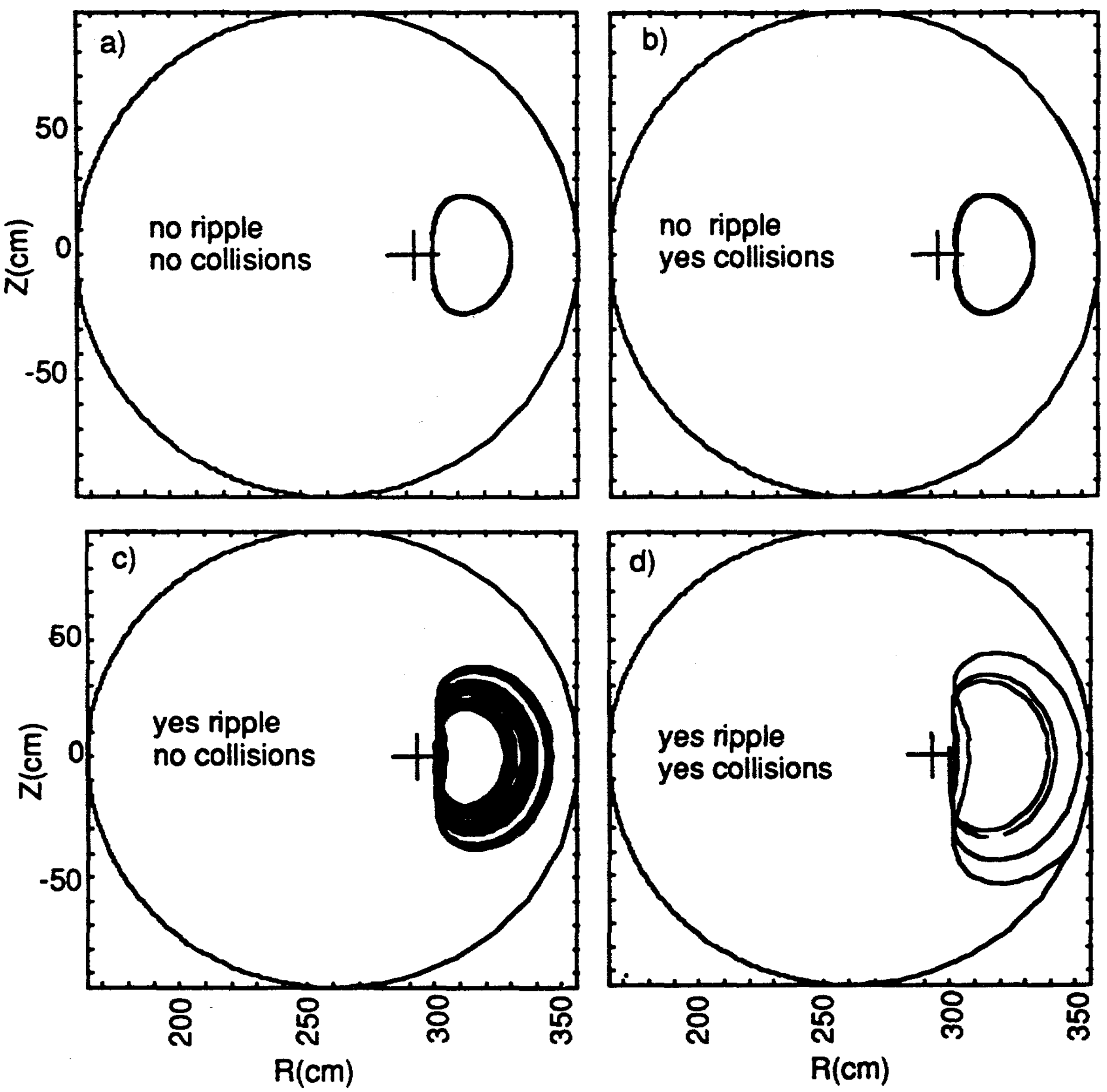
a)
no ripple
no collisions
b)
no ripple
yes collisions
c)
yes ripple
no collisions
d)
yes ripple
yes collisions
Z(cm)
50
0
-50
R(cm)
200
250
300
350

Fig. 8

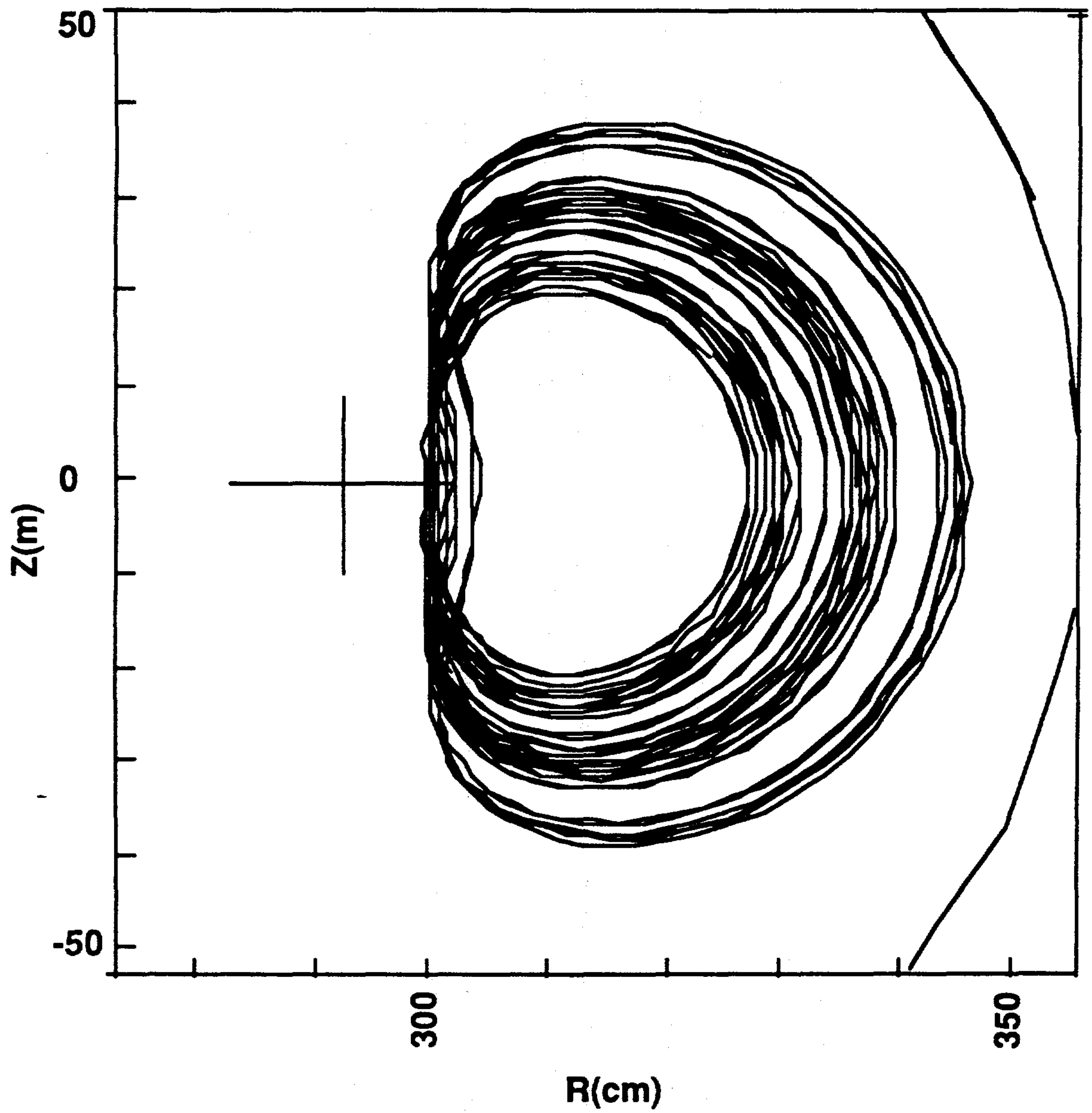

Fig. 9

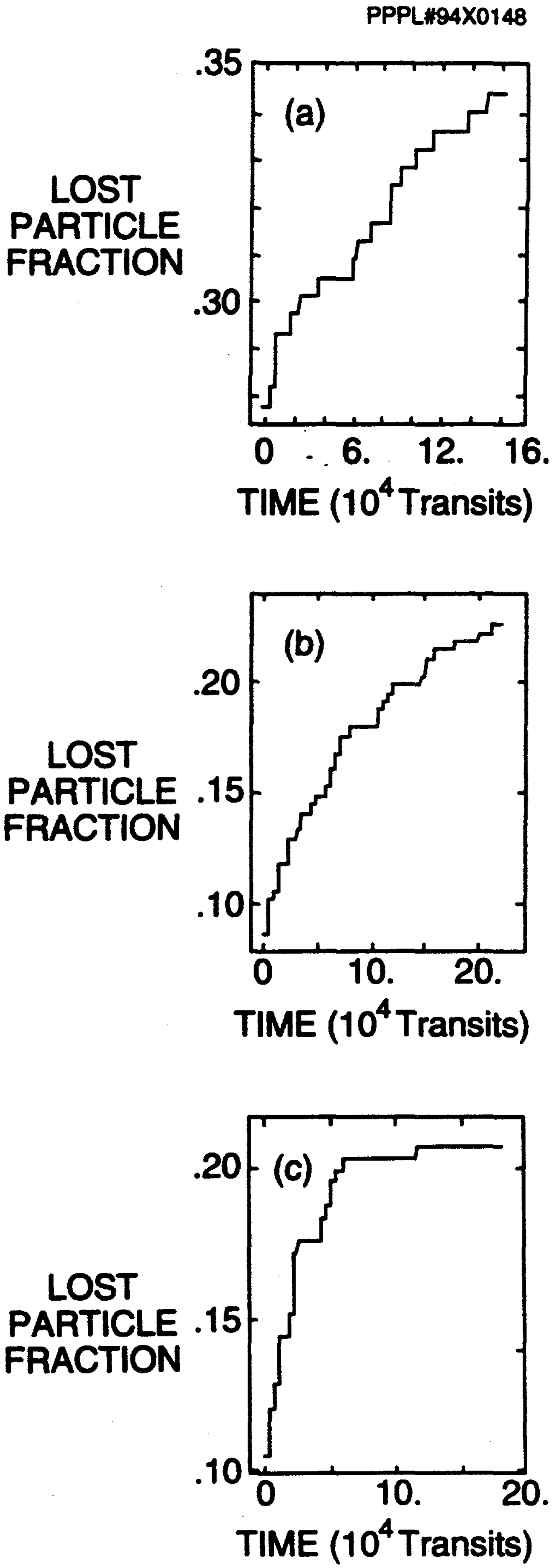
PPPL#94X0148
(a)
LOST PARTICLE FRACTION
.35
.30
0
6.
12.
16.
TIME (10^4 Transits)
(b)
LOST PARTICLE FRACTION
.20
.15
.10
0
10.
20.
TIME (10^4 Transits)
(c)
LOST PARTICLE FRACTION
.20
.15
.10
0
10.
20.
TIME (10^4 Transits)

Fig. 10

PPPL#94X0152

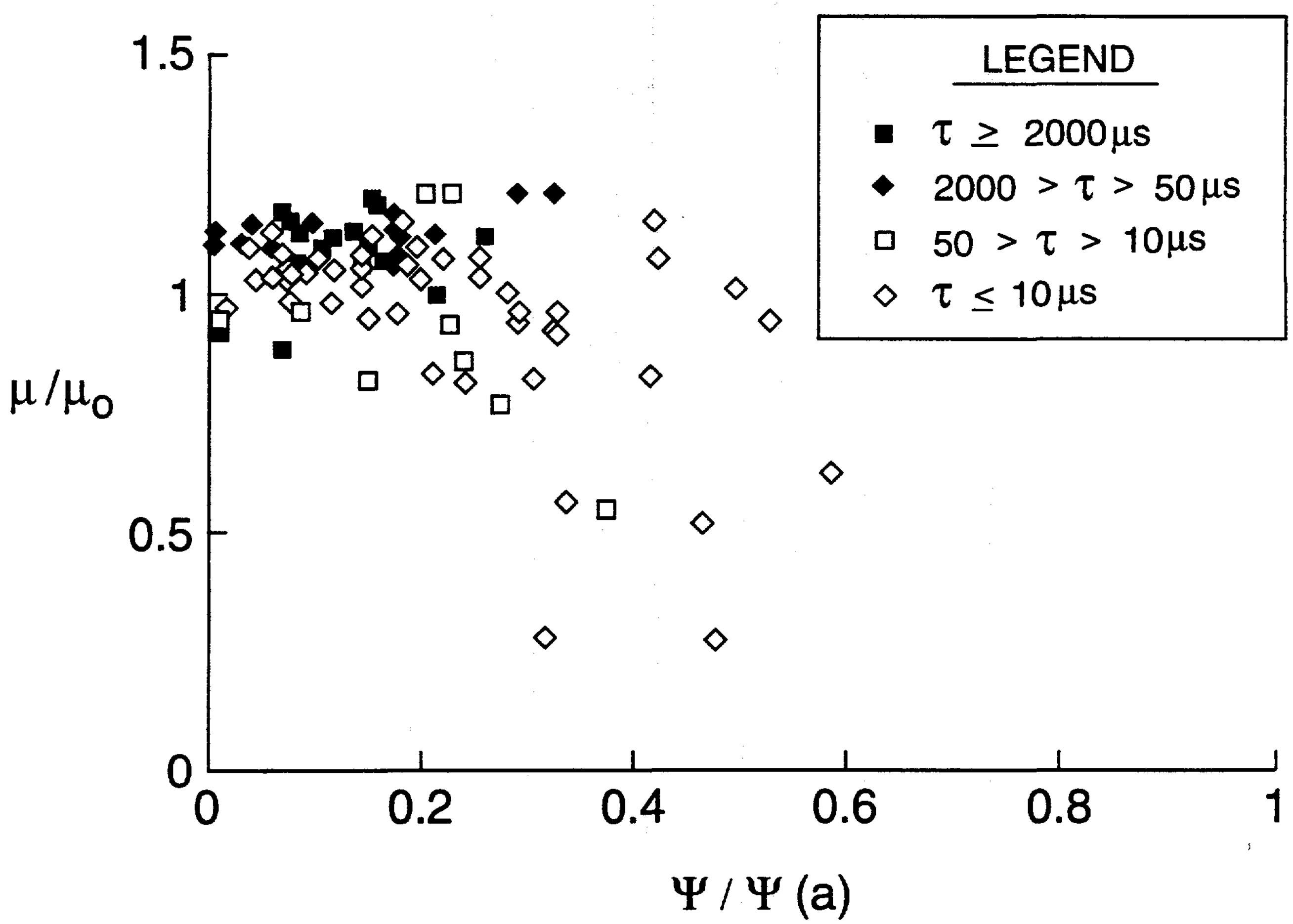

Fig. 11

PPPL#94X0153

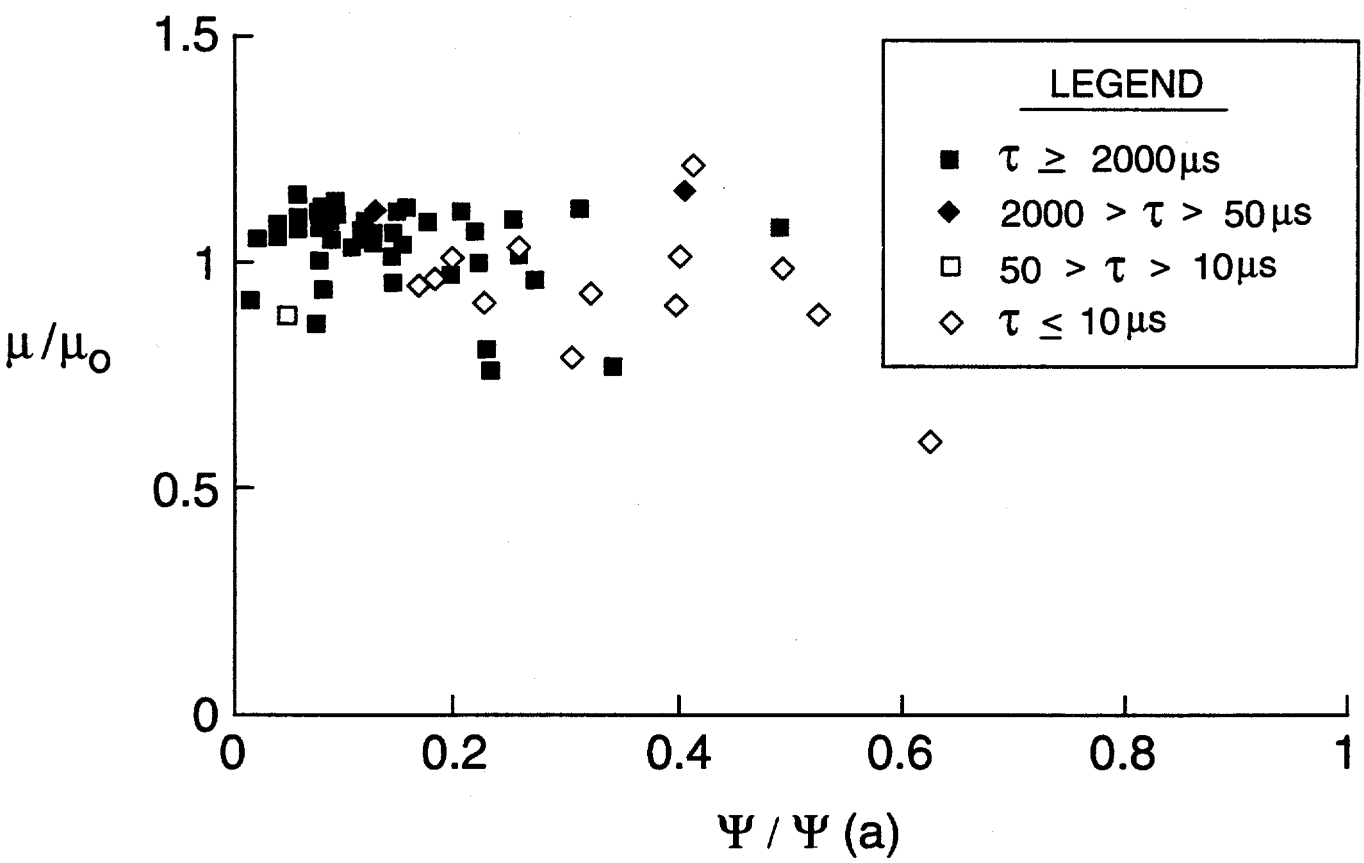

Fig. 12

PPPL#94X0154

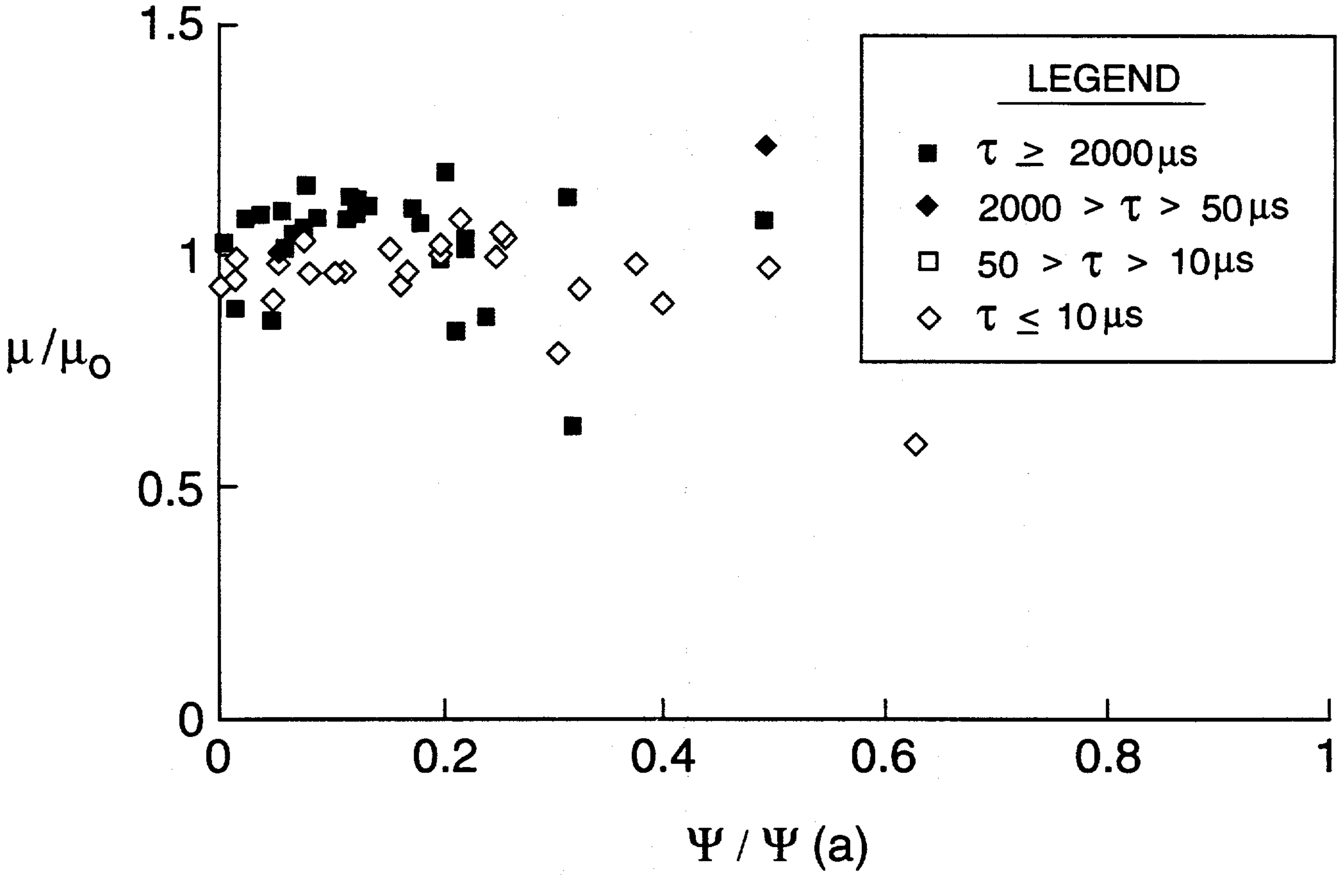

Fig. 13

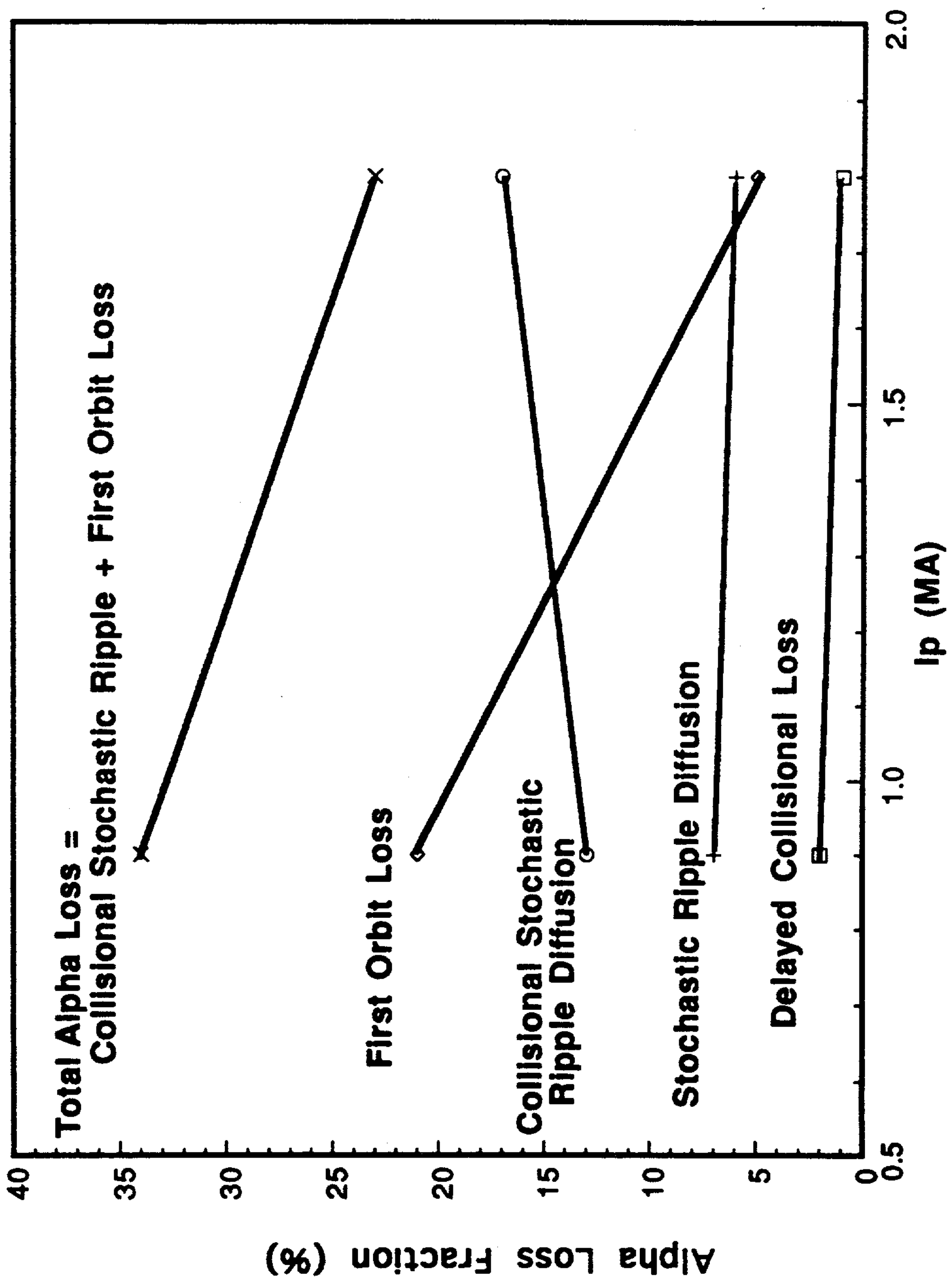
Total Alpha Loss =
Collisional Stochastic Ripple + First Orbit Loss
First Orbit Loss
Collisional Stochastic
Ripple Diffusion
Stochastic Ripple Diffusion
Delayed Collisional Loss
Alpha Loss Fraction (%)
0
5
10
15
20
25
30
35
40
Ip (MA)
0.5
1.0
1.5
2.0

Fig. 14

PPPL#94X0150

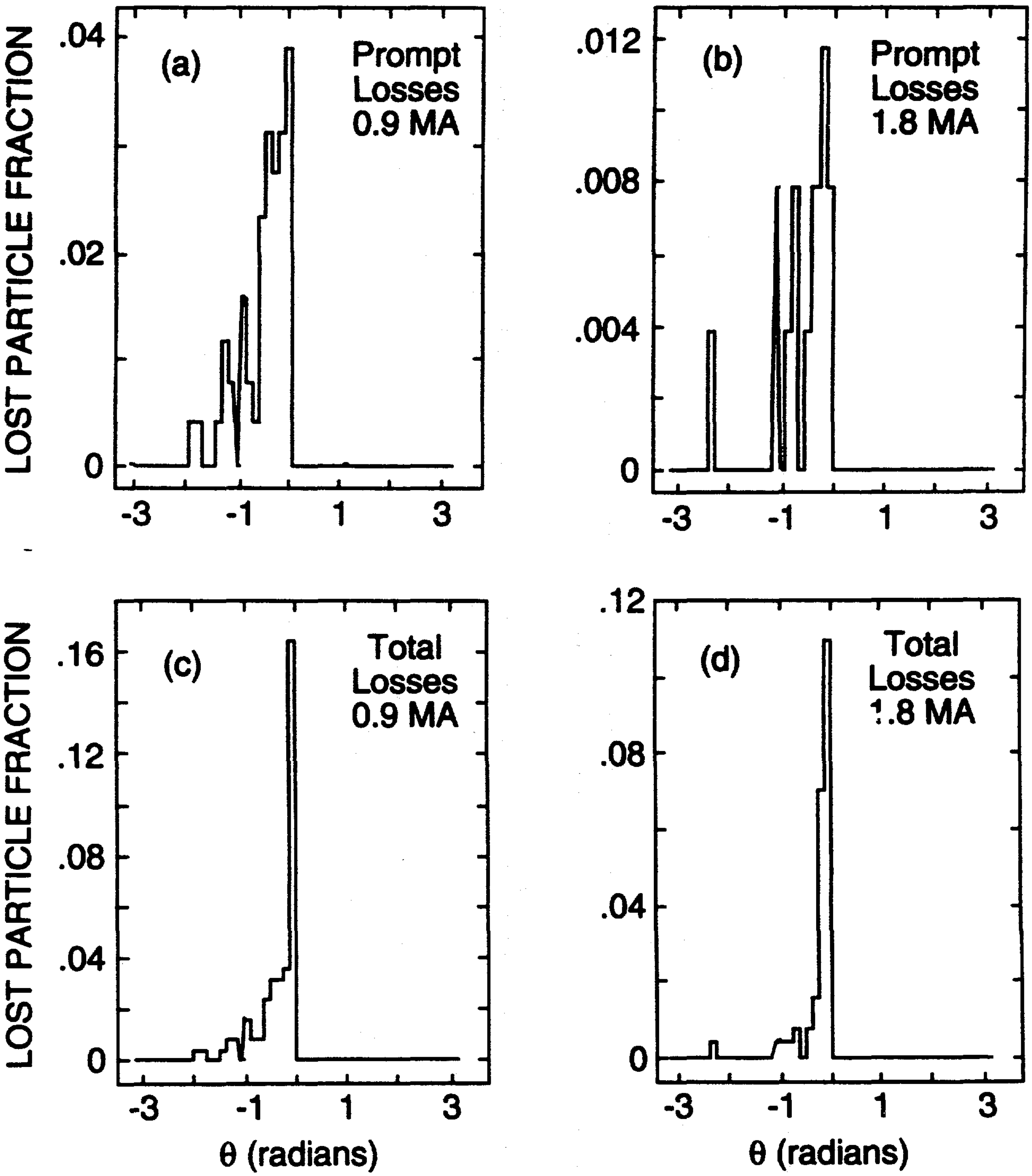

Fig. 15

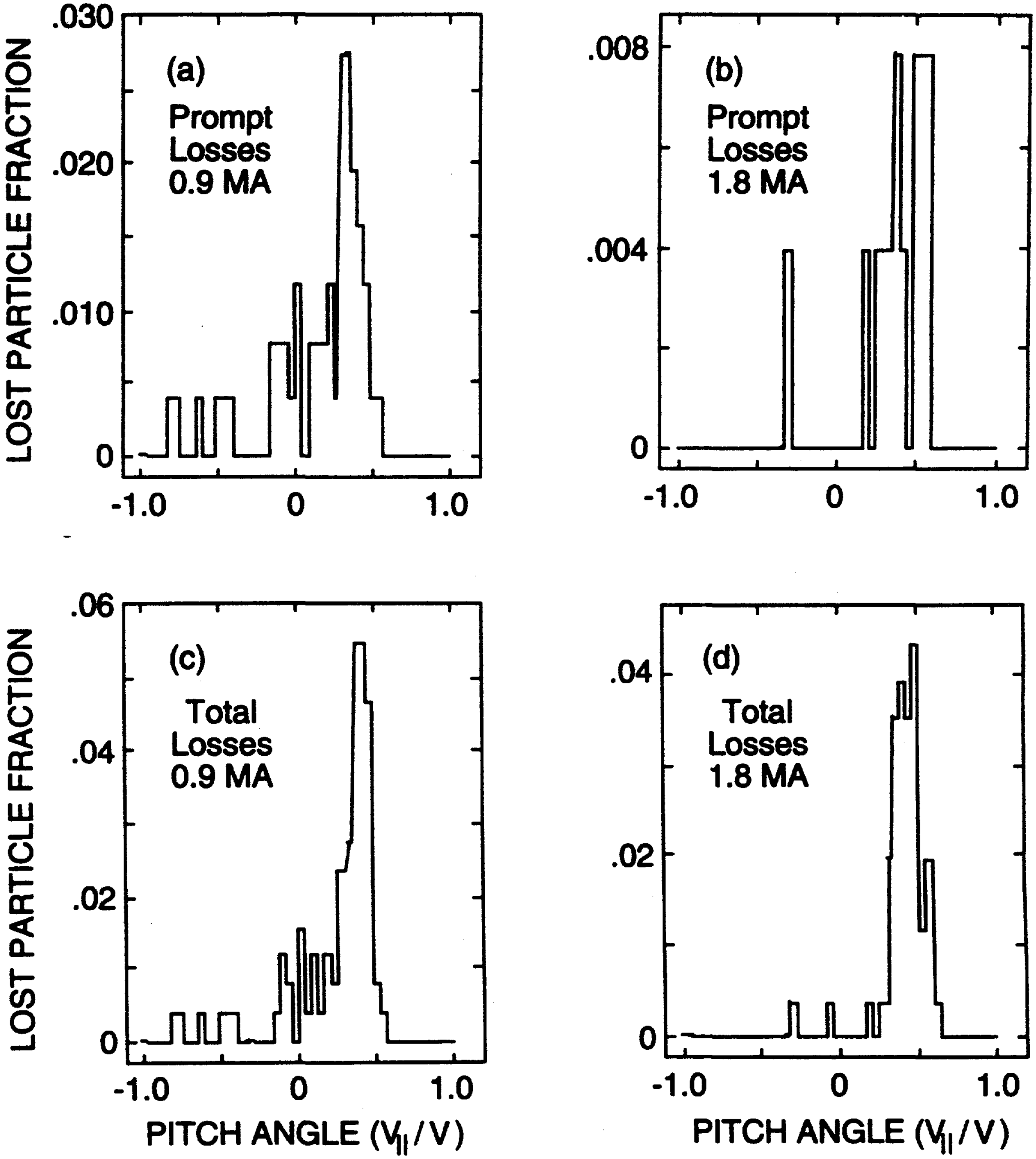
LOST PARTICLE FRACTION
.030
.020
.010
0
(a)
Prompt
Losses
0.9 MA
-1.0
0
1.0
.008
.004
0
(b)
Prompt
Losses
1.8 MA
-1.0
0
1.0
LOST PARTICLE FRACTION
.06
.04
.02
0
(c)
Total
Losses
0.9 MA
-1.0
0
1.0
PITCH ANGLE (V|| / V)
.04
.02
0
(d)
Total
Losses
1.8 MA
-1.0
0
1.0
PITCH ANGLE (V|| / V)

Fig. 16

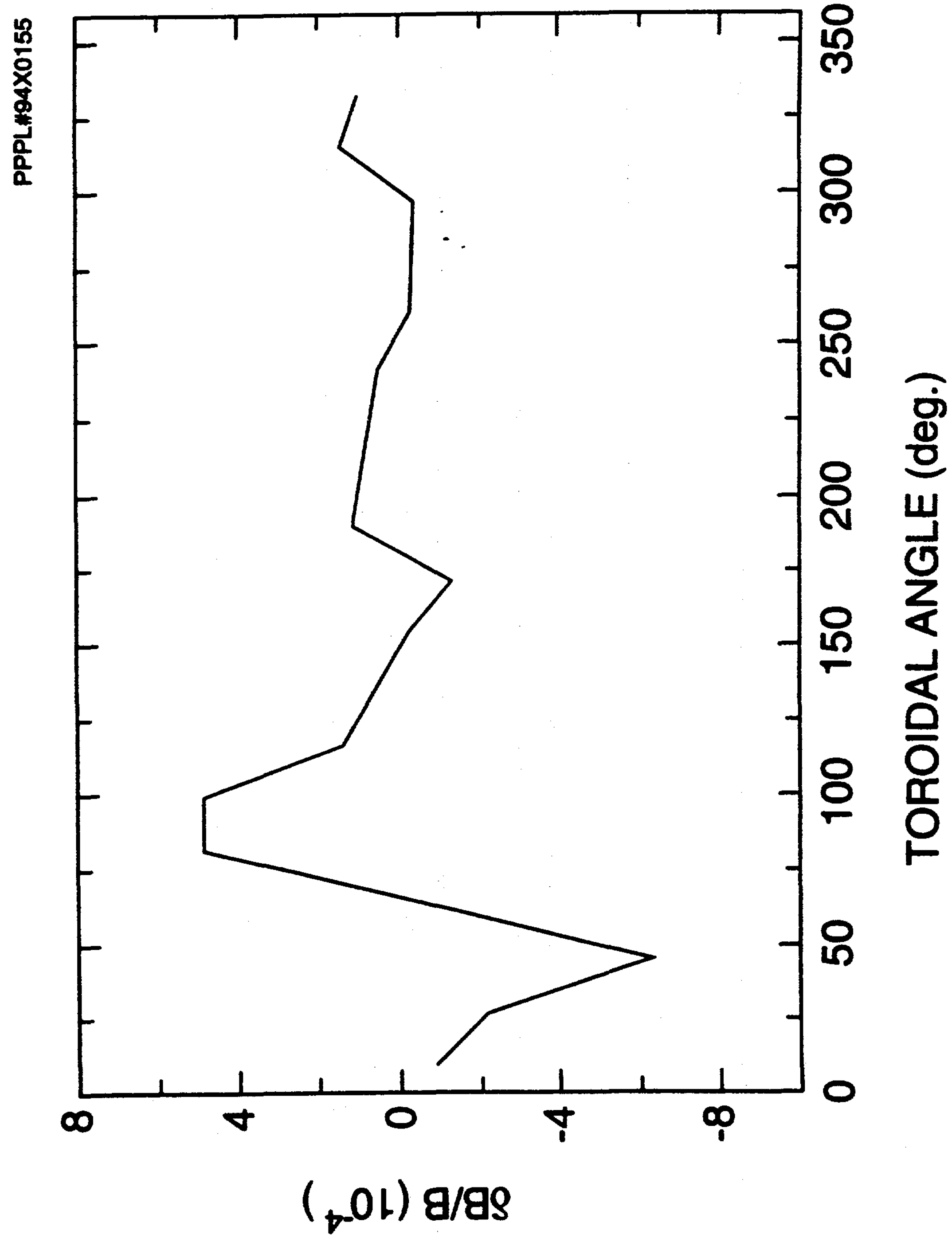
PPPL#94X0155
8
4
0
-4
-8
δB/B (10^-4)
0
50
100
150
200
250
300
350
TOROIDAL ANGLE (deg.)

Fig. 17

EXTERNAL DISTRIBUTION IN ADDITION TO UC-420

Dr. F. Paoloni, Univ. of Wollongong, AUSTRALIA
Prof. R.C. Cross, Univ. of Sydney, AUSTRALIA
Plasma Research Lab., Australian Nat. Univ., AUSTRALIA
Prof. I.R. Jones, Flinders Univ, AUSTRALIA
Prof. F. Cap, Inst. for Theoretical Physics, AUSTRIA
Prof. M. Heindler, Institut für Theoretische Physik, AUSTRIA
Prof. M. Goossens, Astronomisch Instituut, BELGIUM
Ecole Royale Militaire, Lab. de Phy. Plasmas, BELGIUM
Commission-European, DG. XII-Fusion Prog., BELGIUM
Prof. R. Boucique, Rijksuniversiteit Gent, BELGIUM
Dr. P.H. Sakanaka, Instituto Fisica, BRAZIL
Prof. Dr. I.C. Nascimento, Instituto Fisica, Sao Paulo, BRAZIL
Instituto Nacional De Pesquisas Espaciais-INPE, BRAZIL
Documents Office, Atomic Energy of Canada Ltd., CANADA
Ms. M. Morin, CCFM/Tokamak de Varennes, CANADA
Dr. M.P. Bachynski, MPB Technologies, Inc., CANADA
Dr. H.M. Skarsgard, Univ. of Saskatchewan, CANADA
Prof. J. Teichmann, Univ. of Montreal, CANADA
Prof. S.R. Sreenivasan, Univ. of Calgary, CANADA
Prof. R. Marchand, INRS-Energie et Materiaux, CANADA
Dr. R. Bolton, Centre canadien de fusion magnétique, CANADA
Dr. C.R. James,, Univ. of Alberta, CANADA
Dr. P. Lukác, Komenského Universzita, CZECHO-SLOVAKIA
The Librarian, Culham Laboratory, ENGLAND
Library, R61, Rutherford Appleton Laboratory, ENGLAND
Mrs. S.A. Hutchinson, JET Library, ENGLAND
Dr. S.C. Sharma, Univ. of South Pacific, FIJI ISLANDS
P. Mähönen, Univ. of Helsinki, FINLAND
Prof. M.N. Bussac, Ecole Polytechnique,, FRANCE
C. Mouttet, Lab. de Physique des Milieux Ionisés, FRANCE
J. Radet, CEN/CADARACHE - Bat 506, FRANCE
Prof. E. Economou, Univ. of Crete, GREECE
Ms. C. Rinni, Univ. of Ioannina, GREECE
Preprint Library, Hungarian Academy of Sci., HUNGARY
Dr. B. DasGupta, Saha Inst. of Nuclear Physics, INDIA
Dr. P. Kaw, Inst. for Plasma Research, INDIA
Dr. P. Rosenau, Israel Inst. of Technology, ISRAEL
Librarian, International Center for Theo Physics, ITALY
Miss C. De Palo, Associazione EURATOM-ENEA , ITALY
Dr. G. Grosso, Istituto di Fisica del Plasma, ITALY
Prof. G. Rostangni, Istituto Gas Ionizzati Del Cnr, ITALY
Dr. H. Yamato, Toshiba Res & Devel Center, JAPAN
Prof. I. Kawakami, Hiroshima Univ., JAPAN
Prof. K. Nishikawa, Hiroshima Univ., JAPAN
Librarian, Naka Fusion Research Establishment, JAERI, JAPAN
Director, Japan Atomic Energy Research Inst., JAPAN
Prof. S. Itoh, Kyushu Univ., JAPAN
Research Info. Ctr., National Instit. for Fusion Science, JAPAN
Prof. S. Tanaka, Kyoto Univ., JAPAN
Library, Kyoto Univ., JAPAN
Prof. N. Inoue, Univ. of Tokyo, JAPAN
Secretary, Plasma Section, Electrotechnical Lab., JAPAN
Dr. O. Mitarai, Kumamoto Inst. of Technology, JAPAN
Dr. G.S. Lee, Korea Basic Sci. Ctr., KOREA
J. Hyeon-Sook, Korea Atomic Energy Research Inst., KOREA
D.I. Choi, The Korea Adv. Inst. of Sci. & Tech., KOREA
Leandro Melendez Lugo, Inst. Nac'l. de Inves. Nucl, MEXICO
Prof. B.S. Liley, Univ. of Waikato, NEW ZEALAND
Inst of Physics, Chinese Acad Sci PEOPLE'S REP. OF CHINA
Library, Inst. of Plasma Physics, PEOPLE'S REP. OF CHINA
Tsinghua Univ. Library, PEOPLE'S REPUBLIC OF CHINA
Z. Li, S.W. Inst Physics, PEOPLE'S REPUBLIC OF CHINA
Prof. J.A.C. Cabral, Instituto Superior Tecnico, PORTUGAL
Prof. M.A. Hellberg, Univ. of Natal, S. AFRICA
Prof. D.E. Kim, Pohang Inst. of Sci. & Tech., SO. KOREA
Prof. C.I.E.M.A.T, Fusion Division Library, SPAIN
Dr. L. Stenflo, Univ. of UMEA, SWEDEN
Library, Royal Inst. of Technology, SWEDEN
Prof. H. Wilhelmson, Chalmers Univ. of Tech., SWEDEN
Centre Phys. Des Plasmas, Ecole Polytech, SWITZERLAND
Bibliotheek, Inst. Voor Plasma-Fysica, THE NETHERLANDS
Asst. Prof. Dr. S. Cakir, Middle East Tech. Univ., TURKEY
Dr. V.A. Glukhikh,Sci. Res. Inst. Electrophys.I Apparatus, USSR
Dr. D.D. Ryutov, Siberian Branch of Academy of Sci., USSR
Dr. G.A. Eliseev, I.V. Kurchatov Inst., USSR
Librarian, The Ukr.SSR Academy of Sciences, USSR
Dr. L.M. Kovrizhnykh, Inst. of General Physics, USSR
Kernforschungsanlage GmbH, Zentralbibliothek, W. GERMANY
Bibliothek, Inst. Für Plasmaforschung, W. GERMANY
Prof. K. Schindler, Ruhr-Universität Bochum, W. GERMANY
Dr. F. Wagner, (ASDEX), Max-Planck-Institut, W. GERMANY
Librarian, Max-Planck-Institut, W. GERMANY